SPECTROSCOPY AND CHEMISTRY OF THE ATMOSPHERE OF URANUS

BRUCE FEGLEY, JR.
Max-Planck-Institut für Chemie

DANIEL GAUTIER
Observatoire de Paris-Meudon

TOBIAS OWEN
University of Hawaii

and

RONALD G. PRINN
Massachusetts Institute of Technology

We give a comprehensive review of the chemistry and spectroscopy of the atmosphere of Uranus. Earth-based, Earth-orbital, and Voyager 2 observations covering the ultraviolet, visible, infrared and radio wavelength regions are discussed. This suite of observations, in concert with the average density of ~ 1.3 *g* cm^{-3} *imply that the atmosphere of Uranus is enriched in heavy elements* ($Z \geq 3$) *relative to solar composition. In particular, pre-Voyager Earth-based observations of* CH_4 *bands in the visible region and Voyager 2 radio occultation data imply a* CH_4/H_2 *volume mixing ratio of about 2% corresponding to an enrichment of approximately 24 times the solar value of* 8.35×10^{-4}. *The Earth-based spectroscopic data of Lutz et al. imply that this enrichment may be as small as 17 times solar or as large as 42 times solar. However, in contrast to* CH_4, *microwave observations indicate an apparent depletion of* NH_3 *in the 150 to 200 K region of the atmosphere by 100 to 200 times relative to the solar* NH_3/H_2 *mixing ratio of* 1.74×10^{-4}. *The temporal and latitudinal variations*

In *Uranus* (1991), J. Bergstrahl, E. Miner, and M. S. Matthews, Eds. University of Arizona Press, Tucson.

deduced for the NH_3/H_2 mixing ratio in this region of the Uranian atmosphere may be due to atmospheric circulation effects. Attempts to explain the low NH_3 abundance in terms of physical effects (e.g., the failure of Uranus to have accreted nitrogen-bearing gas and grains) and chemical effects (NH_3 solubility in low-lying aqueous solution clouds and/or removal by NH_4SH cloud formation) are also reviewed. Both classes of explanations suffer from problems that prevent uncritical acceptance. In particular, several of the published NH_3 solubility calculations are based upon incorrect extrapolation of thermodynamic data to the high temperatures predicted for water cloud condensation on Uranus. Thus, the exact reason(s) for the deduced NH_3 depletion remains obscure. The He mole fraction of 15.2 ± 3.3% determined by Voyager 2 suggests that helium differentiation has not occurred on Uranus. The He/H_2 ratio observed on Uranus may therefore be representative of the primitive solar nebula. The D to H ratio derived from CH_3D observations and a fractionation factor of ~ 1.3 is ~ 7×10^{-5}, which is higher than that on Jupiter and Saturn ($D/H \sim 2 \times 10^{-5}$). Chemical models imply that both equilibrium and non-equilibrium (e.g., photochemistry and vertical mixing) processes are important on Uranus. In particular, vertical mixing is predicted to be an important source of N_2 in the troposphere of Uranus. Other trace gases which are predicted to be transported upward from the 1000 to 2000 K region of the atmosphere of Uranus include CO, PH_3, GeH_4, AsH_3, HCN, CO_2, C_2H_6, CH_3SH, CH_3NH_2, CH_3OH, H_2Se, HCl and HF. Although the abundance of several of these species may be severely limited by condensation in the cold Uranian upper atmosphere, these gases are potentially detectable by a suitably designed mass spectrometer on an atmospheric entry probe. Finally, we note that for sufficiently large enrichments of the H_2O/H_2 ratio over solar composition (1.38×10^{-3}) water cloud condensation will occur at the water critical point of 647 K. The corresponding H_2O/H_2 mixing ratio is 9%.

I. INTRODUCTION

A large number of different observations show that the atmosphere of Uranus is fundamentally different from the atmospheres of Jupiter and Saturn. The average density of ~ 1.3 g cm^{-3} and interior structure models have long been understood to require that Uranus is enriched in heavy elements ($Z \geq 3$) relative to solar composition (see, e.g., Brown 1950; Hubbard 1984*a*; Reynolds and Summers 1965; Wildt 1961; Podolak and Reynolds 1987; chapter by Podolak et al.). Earth-based spectroscopic observations of CH_4 in the visible and near-infrared regions imply CH_4/H_2 mixing ratios of 1% to 10% (Baines 1983; Bergstralh and Baines 1984; Lutz et al. 1976; Wallace 1980) and Voyager 2 radio-occultation measurements imply a CH_4/H_2 mixing ratio of approximately 2% (Lindal et al. 1987). Earth-based (see, e.g., Fazio et al. 1976; Loewenstein et al. 1977; Moseley et al. 1985) and Voyager 2 (Pearl et al. 1990; chapter by Conrath et al.) thermal radiance observations imply approximate equilibrium with absorbed sunlight and the absence of a significant internal heat source. The thermal radiance observations also imply that the deep atmosphere of Uranus is colder and denser (i.e., greater pressure at a given temperature) than the atmospheres of Jupiter and Saturn. Finally, microwave spectra indicate an apparent depletion of NH_3 in the 150 to 200 K

region of the atmosphere of Uranus by 100 to 200 times relative to the solar NH_3/H_2 mixing ratio of 1.74×10^{-4} (de Pater and Massie 1985; de Pater and Gulkis 1988; Gulkis et al. 1978,1983; Klein and Turegano 1978; de Pater et al. 1989; Hofstadter and Muhleman 1989).

Taken together, these observations appear to raise more questions than they answer. For example, why is one hydride (CH_4) enriched by about 24 times over the solar C/H_2 ratio while another hydride (NH_3) is apparently depleted 100 to 200 times below the solar N/H_2 ratio? Also, aside from sometimes contradictory spectroscopic observations of CH_4 in the visible and near-infrared regions and of H_2 quadrupole and dipole transitions, there are no direct observations of any other chemical species in the troposphere of Uranus. This situation is drastically different from that on Jupiter and Saturn where a wealth of compositional data are available from visible and infrared spectroscopy of the tropospheres of these two planets (e.g., see the recent review by Gautier and Owen [1989]).

In this chapter, we review the Earth-based, Earth-orbital and Voyager 2 observations of the atmosphere of Uranus with an emphasis on spectroscopic observations of the troposphere. The chapter by Atreya et al. reviews observational data and photochemical models relevant to the stratosphere of Uranus, and the chapter by Podolak et al. focuses on the deep interior (roughly on the region with $T > 2000$ K). After a comprehensive review of the spectroscopic observations, we discuss the implications of chemical models for the equilibrium and nonequilibrium chemistry of the troposphere of Uranus. Our discussion of equilibrium chemistry includes a discussion of cloud condensation chemistry (primarily for the species H_2O, NH_3 and H_2S) which complements the review in the chapter by West et al. of clouds and aerosols in the observable regions of the atmosphere of Uranus. Finally, we conclude this chapter by summarizing the important observational and theoretical problems which need to be addressed in future investigations.

II. ATMOSPHERIC STRUCTURE

The thermal structure of the observable part of the atmosphere of Uranus is similar to those of the other giant planets. Figure 1 exhibits the temperature profile in the equatorial region of the planet inferred from Voyager radio occultations (Lindal et al. 1987). This similarity was expected since the radiative opacity as well as the sources and sinks of energy are similar in the four giant planets (Appleby 1986). The opacity in the far infrared range where the planetary thermal emission peaks is dominated by the $H_2 - H_2$ and $H_2 - He$ collision induced absorption (Fig. 2) and is responsible for the thermal structure of the upper troposphere. The near infrared solar energy is absorbed at stratospheric levels by methane and by aerosols, leading to a temperature inversion. Uranus is peculiar, however, in several respects. First, the low-temperature tropopause acts as an efficient cold trap and limits the

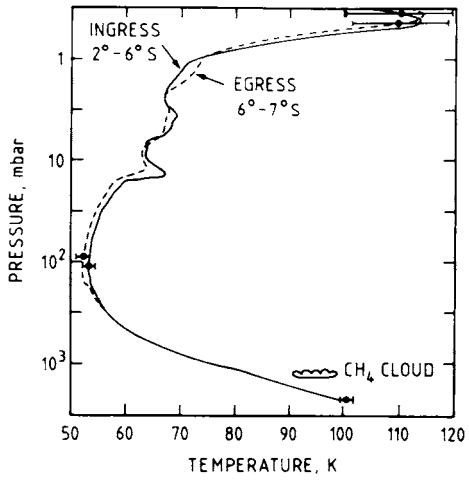

Fig. 1. Uranian temperature-pressure profiles derived from the Voyager 2 radio occultation measurements (figure after Lindal et al. 1987).

abundance of methane in the stratosphere, so that the temperature inversion is less pronounced than in the other three giant planets. Aerosols appear to compensate partially the methane deficiency, however, and are believed to be responsible for the relatively high temperature observed around the 0.5 mbar pressure level. Second, the internal energy of Uranus is quite small. From Voyager infrared observations, Pearl et al. (1990) estimate this energy to be less than 1.14 times the absorbed solar flux with the most plausible value equal to 1.06. Such a low value implies rather weak convection in the deep troposphere of the planet which may result in a subadiabatic lapse rate at some levels (Bézard and Gautier 1986; Friedson and Ingersoll 1987). This may in turn limit the efficiency of the upward mixing of nonequilibrium gases from the deep atmosphere (Fegley and Prinn 1985*b*, 1986).

Another interesting aspect is the near absence of latitudinal temperature variations in the troposphere (Flasar et al. 1987) that requires the occurrence of a dynamical redistribution of heat between equator and pole (Friedson and Ingersoll 1987). However, latitudinal temperature variations do occur in the stratosphere, as the temperature inferred at the 2.7 mbar level from the ultraviolet occultation experiment near 67 N is about 15 K warmer than the equatorial temperature at the same level (West et al. 1987).

The most obvious result of the low tropopause temperature of Uranus (53 K) is that most volatiles condense at this level and cannot penetrate into the stratosphere in substantial amounts. However, hydrocarbons and possibly complex polymers may be formed from the photochemistry of methane in this region of the atmosphere (Smith et al. 1986; Pollack et al. 1987; Khare et al. 1987).

As noted above, the apparent lack of a significant internal heat source

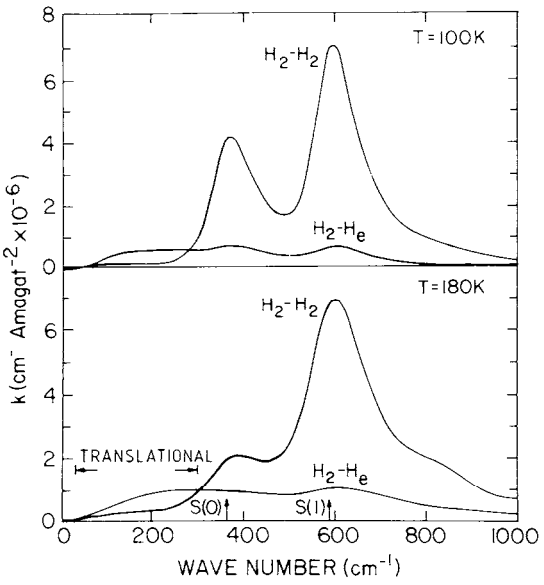

Fig. 2. Pressure-induced absorption coefficients k for $H_2 - H_2$ and $H_2 - He$ collisions at Saturn-like temperatures (100 K) and Jupiter-like temperatures (180 K) (figure after Gautier et al. 1981).

on Uranus makes the assumption of an adiabatic gradient in the deep atmosphere debatable. Nevertheless, the remaining primordial heat escaping from Uranus, which Hubbard (1978) estimated as approximately 100 erg cm^{-2} s^{-1} (or about 15% of the absorbed solar flux of ~ 650 erg cm^{-2} s^{-1}), is apparently sufficient to maintain convection throughout the atmosphere (e.g., see Wallace 1980). Also, thermal emission from the deep atmosphere with temperature increasing with depth is the preferred model to explain the observed microwave spectra (Gulkis and de Pater 1984). For these reasons interior structure models (see, e.g., Hubbard 1984*a;* Podolak et al. 1985; chapter by Podolak et al.) assume an adiabatic gradient. In our discussion in this chapter of the chemistry of the atmosphere of Uranus we specifically assume that the temperature gradient in the atmosphere beneath the radiative convective boundary is adiabatic throughout. A more detailed discussion of the thermal structure of the atmosphere of Uranus can be found in the chapter by Conrath et al.; the implications for the dynamics and circulation of the atmosphere are discussed in the chapter by Allison et al.

III. SPECTROSCOPIC STUDIES OF URANUS

A. Early History

The record of spectroscopic studies of Uranus is long and confused, full of errors and frustrations. From our present vantage point, it appears that

much of the early confusion could be attributed to the unusual transparency of the planet's atmosphere. Compared with Jupiter and Saturn, the absence of thick clouds in the upper troposphere of Uranus means that the optical paths responsible for the visible and the near-infrared spectrum correspond to much larger linear distances through the planet's atmosphere. Hence, gaseous absorptions were found in the spectrum of Uranus that were not present in spectra of its larger neighbors. These absorptions had never been seen in the laboratory and were in fact not easy to reproduce there. It turned out eventually that they were caused by forbidden transitions of hydrogen and high-frequency combination bands of methane.

The problems involved in the interpretation of these features were exacerbated by the basic difficulty posed by the planet's faintness and small apparent size. Spectroscopic studies of Uranus have always been difficult and observations of center-to-limb effects nearly impossible. Atmospheric models that attempted to include the scattering properties of the aerosols that were present were therefore not well constrained. Despite all this, it was apparent from the start that the atmospheres of both Uranus and Neptune are very different from those of Jupiter and Saturn.

The first observations of the spectrum of Uranus were made by visual observers in the 19th century. Both Secchi (1869) and Huggins (1871) reported the presence of strong bands in the visible spectra of both Uranus and Neptune, extending to the green and blue regions. These bands were not present in any other astronomical sources and their identity was a puzzle. There was even some discussion as to whether the appearance of the spectra of these two planets might actually be the result of emission features rather than absorption bands.

The development of the photographic emulsion, which was gradually sensitized to longer and longer wavelengths by the application of special dyes, enabled subsequent observers to discover many additional absorptions. The most active observer during this era was V. M. Slipher of the Lowell Observatory. In 1932, he summarized thirty years of studies of planetary spectra in the George Darwin Lecture of the Royal Astronomical Society (Slipher 1933). While Slipher described his observations in detail, noting that the intensities of bands in the red region increased with the increasing distance of the major planets, R. Wildt at Göttingen was the first person to identify these absorptions. Using Slipher's spectra as well as some of his own, Wildt (1932) suggested that the bands at 5430 Å, 6190 Å, 7260 Å, 8650 Å and 8900 Å were caused by methane. He made these identifications by extrapolating from the only short wavelength methane band observed in the laboratory, the one at 8900 Å (Dennison and Ingram 1931), using a formula developed by these latter authors for the prediction of the position of overtones of the ν_3 fundamental at 3.3 μm.

The identifications were extended by Adel and Slipher (1934) who employed a double-traversal absorption cell with a length of 22.5 meters that

could be pressurized to 45 atmospheres. They used this cell to study spectra of methane, ethane and ethylene. They concluded that all of the methane bands they could observe in the laboratory were present in the planetary spectra and that the total column abundance of this gas corresponding to the planetary spectra was 3.2 km atmospheres, an extrapolation from the largest column density they achieved. However, both Uranus and Neptune exhibited additional bands in the blue and green region (the ones discovered by Secchi and Huggins) that Adel and Slipher were unable to reproduce with their absorption cell. They remarked that even the strongest of the ethylene and ethane bands that they also observed with this apparatus were not present in the planetary spectra, but they did not try to set any abundance limits.

Herzberg (1945,1952*a*) criticized the early attempts at identifications and abundance determinations on the grounds that the data were inadequate to support general formulae for the frequencies of overtone and combination bands and the laboratory studies were carried out at pressures too high to match realistic conditions in the planetary atmospheres. The fact that the identified bands were caused by methane was not challenged, it was a question of which methane bands they were, and how much methane was really required to produce them. Modifying a design originally proposed by White (1942), Herzberg constructed multiple-path absorption cells at the Yerkes Observatory in which the light could make a larger number of traversals through the gas being studied before leaving the cell for spectrographic analysis. Thus, a long path length could be achieved at low pressure. This became the accepted procedure for laboratory studies from that time onward.

Kuiper (1952) had been extending the work of Slipher by employing the coudé spectrograph of the 82-in telescope at the McDonald Observatory to photograph planetary spectra at higher resolution than previous workers were able to obtain. He used the long absorption cell built by Herzberg to record methane spectra for comparison with his spectra of the outer planets. Choosing the weakest methane band he could identify in the spectrum of Uranus, he deduced a column abundance of 2.20 km amagat for the abundance of methane in the spectroscopically accessible region of the Uranus atmosphere. However, his laboratory spectra still did not reproduce the green and blue bands in the planet's spectrum.

Among the first results Herzberg himself achieved with the Yerkes absorption cell was the observation of the H_2 quadrupole lines (Herzberg 1952*a*), whose spectrum he had correctly predicted 14 yr earlier (Herzberg 1938). Subsequently at Ottawa, using a shorter cell that could be highly pressurized and cooled, Herzberg (1952*a*) also recorded the 3–0 H_2 pressure-induced dipole spectrum. He further showed that an unidentified absorption found by Kuiper (1952) in the spectrum of Uranus at 8258 Å was in fact caused by the pressure-induced 3–0 S(1) line of H_2. This was the first identification of hydrogen in the atmosphere of any giant planet, the first identification of molecular hydrogen in any astronomical source.

In addition to the feature at 8258 Å, Kuiper (1952) found several lines near 7800 Å in the spectrum of Uranus that were also not present in the laboratory spectra of methane. Several attempts to identify these features led to negative results (see, e.g., Bardwell and Herzberg 1953), until Owen (1967), using longer path lengths than previous workers, discovered that they were in fact caused by methane. Owen emphasized that the maximum path length he had achieved in the laboratory, corresponding to the column density of 1.7 km amagat of methane on Uranus, was still not sufficient to match the *intensities* of the 7800 Å bands, even though it was adequate to make the identification. He suggested that the column abundance of methane on Uranus was still underestimated, even though it was now clear that it must be considerably greater than the value proposed by Kuiper (1952).

B. Results Since 1970

Work done during the first decade of this period has been discussed in a detailed review by Trafton (1981) (also see Belton 1982 and Bergstralh and Baines 1984). Here we shall try to use the perspective provided by the Voyager 2 encounter to follow the developing understanding of the composition and structure of the atmosphere.

1. Methane. The absence of a specific identification of the green and blue bands in the Uranus and Neptune spectra led Danielson (1974) to propose that they were caused by simultaneous transitions produced during methane-hydrogen collisions. However, Owen and Cess (1975) pointed out that at least two of these bands were weakly present in the atmosphere of Jupiter and thus were probably caused by methane itself. This allowed the use of a band model to predict methane path lengths on Uranus, given the measured strengths of the absorption there (Galkin et al. 1971) and the abundance deduced on Jupiter. The results suggested path lengths of several km amagat of CH_4 and a mixing ratio of CH_4/H_2 over 1%. Clearly what was needed to obtain more precise values of $N[CH_4]$ was a systematic laboratory study of methane using still longer optical paths. The first such program was carried out by Lutz et al. (1976) making use of the 33 m White cell built by D. A. Ramsay at the Herzberg Institute for Astrophysics. Previously, Lutz and Ramsay (1972) had used a path length of 10 km amagat of methane with the cell to confirm Owen's (1967) identification of the 7800 Å bands. Now 15 different pressure-path length combinations were employed to develop curves of growth, up to a maximum column density of 9.3 km amagat. With these spectra, Lutz et al. (1976) were able to demonstrate conclusively that the green and blue bands are also vibration-rotation bands of methane, requiring column densities of 5 km amagat to become visible. They derived a column abundance of $5.8^{+0.4}_{-1.0}$ km amagat for methane on Uranus, using their curves of growth and band strengths for these bands. In the process, Lutz et

al. (1976) discovered that the growth of absorption in these combination bands was independent of pressure, since the individual lines are so closely packed. These results were subsequently confirmed and extended by Fink et al. (1977), Giver (1978) and Lutz et al. (1982).

Owen (1966) had called attention to a methane band with unusually regular structure near 6800 Å that he attributed to the 4th overtone of ν_3. This allowed the assignment of quantum numbers to the "lines" in the band, but the spectral resolution was too low to verify that these features actually consisted of the components appropriate to their J numbers. Several authors subsequently attempted to use this band or "lines" in it to analyze the atmosphere of Uranus. However, Lutz and Owen (1976) showed that it cannot be $5\nu_3$ because the rotational quantum number assignments corresponding to this identification cannot be correct. This conclusion was based on high resolution room temperature laboratory data, showing that the splitting of the manifolds did not follow the rotational quantum numbers and that the derived rotational temperature was 25 K. Despite this analysis, the attribution of $J = 0$ to the 6818.9 Å feature has continued (see, e.g., Baines 1983). Keffer et al. (1986) have now demonstrated that the rotational assignment for this line is more likely in the range $2 < J < 5$, based on low-temperature laboratory spectra. Clearly more work is needed here to establish which (if any) of these lines is a singlet and what their J values are.

Working with entire bands rather than individual lines, Fink and Larson (1979) used their own laboratory spectra of two weak CH_4 bands to interpret a spectrum of Uranus recorded at 3.6 cm^{-1} resolution in the near infrared. They derived a column abundance of 1.6 km amagat for methane on Uranus and suggested that the larger amounts derived from the visible bands were caused by greater multiple scattering at those wavelengths. They regarded their results as ". . . a more realistic estimate of the one-way abundance of methane for the atmospheres of Uranus and Neptune," while emphasizing the limitations of their own analysis.

In retrospect, it seems we were dealing with the classical case of the blind men and the elephant. Different results were being obtained for the methane abundance depending on what region of the spectrum was being analyzed. A common view was not emerging.

2. The He to H_2 Ratio: Observations. The inference of the He/H_2 ratio value from groundbased or even airborne experiments is difficult. Helium exhibits a resonance line at 584 Å, which has been observed on Uranus by Voyager (Broadfoot et al. 1986) but the line is formed very high in the atmosphere above the homopause in a region where H_2 and He are not uniformly mixed.

The only practical method for estimating the He/H_2 ratio results from the analysis of the far infrared spectrum of the planet. Neither helium nor

molecular hydrogen has a permanent dipole moment. H_2 exhibits pure rotational quadrupole lines at long wavelengths up to 28 μm but these lines must be extremely narrow in the atmospheres of the giant planets (Goorvitch and Chackerian 1977) and have not yet been observed. On the other hand, a dipole can be induced during a short period of time when collisions occur between two H_2 molecules or a H_2 molecule and a He atom. The resultant collision induced absorption has an appreciable effect, even at low pressures, because of the very long path lengths encountered in the atmosphere of Uranus and in the atmospheres of the other giant planets.

The formulation used for treating the collision induced absorption of H_2 is summarized in Gautier et al. (1981); a review of the theory can be found in Birnbaum (1978). Spectral variations of the H_2-H_2 and H_2-He absorption coefficients at two different temperatures are shown in Fig. 2. As a consequence of the large abundances of H_2 and He in Uranus, the continuum opacity in the whole infrared and submillimeter range is mainly due to this absorption (Hildebrand et al. 1985; Bézard et al. 1986; Orton et al. 1986).

Only a few lines or bands are superimposed on this continuum. That is due to the fact that the thermal emission originates from the quite cold upper troposphere where most of the species condense so that only a few weak absorption lines are expected (Bézard et al. 1986). Stratospheric emission bands are not too numerous either. Only C_2H_2 has been detected at 12 μm up to now (Orton et al. 1987*b*). On the other hand, calculations of the H_2-He opacity indicate that the planetary emission originates from the same atmospheric level at different wavelengths. That suggests the idea to retrieve the tropospheric temperature profile from a part of the spectrum for various values of the He/H_2 ratio. Calculating synthetic spectra from these profiles in another part of the spectrum, the He/H_2 ratio is inferred from the best fit of the observations. This method was initially attempted by Courtin et al. (1978), using an inversion of the radiative transfer equation applied to available, groundbased observations. They suggested that the He molar abundance should not exceed 20% by volume. More recently, Orton (1986), using new groundbased and aircraft observations, proposed a He abundance of $40 \pm 15\%$ by volume. The difficulty of properly calibrating infrared spectra and removing the telluric opacity makes the method quite hazardous, and this surprisingly high value was not subsequently confirmed by Voyager observations.

The encounter of Voyager 2 with Uranus allowed the application of a more reliable technique, already used with success for deriving the He abundance in Jupiter and Saturn (Gautier et al. 1981; Conrath et al. 1984). This method employs results from two different experiments. The radio-occultation experiment provides the ratio of the temperature over the mean molecular weight, which depends upon the He/H_2 ratio. (In the upper atmosphere of Uranus, methane condenses so that its abundance is quite low. Other possible minor components such as argon, neon, etc. contribute only very

weakly to the mean molecular weight.) From a set of temperature profiles, determined for various values of the He/H_2 ratio (Fig.3), synthetic infrared spectra are then calculated and compared to spectra recorded by the IRIS experiment at the latitude of the occultation points (2° and 6° N). The best fit (Fig.4) corresponds to the value of the He/H_2 ratio in this part of the atmosphere (Conrath et al. 1987).

The method is quite sensitive since the temperature inferred from the radio-occultation data is directly proportional to the mean molecular weight (Fig.3). The uncertainty due to random and calibration errors in the IRIS measurements is negligible. Systematic errors due to uncertainties in the H_2-He and CH_4-H_2 absorption coefficients, in the CH_4 abundance, and a possible cloud opacity are small. The main cause of errors results from uncertainties in the refractivity profile measured by the radio-occultation experiment (Lindal et al. 1987). Taking all uncertainties into account, the helium mole fraction q in the upper troposphere of Uranus has then been found equal to $15.2 \pm 3.3\%$ by volume and the corresponding mass fraction Y is 0.262 ± 0.048 (Conrath et al. 1987).

The interpretation of this result in a cosmogonical perspective raises two questions. The first question is whether the He abundance in the outer layers of Uranus is representative of the value in the bulk of the planet. In other

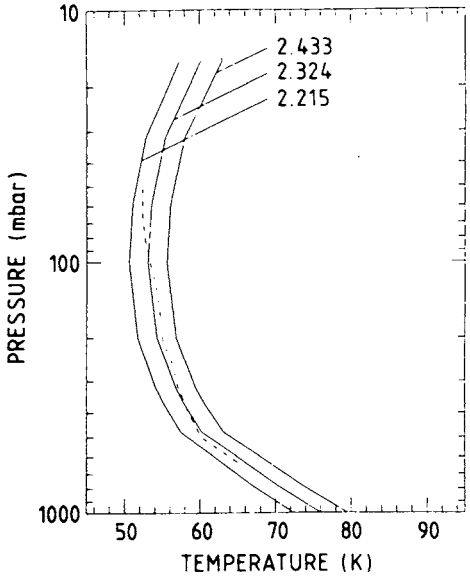

Fig. 3. Uranian temperature-pressure profiles derived from Voyager 2 infrared spectroscopy and radio science observations. The solid curves, which were derived from the radio-occultation data, are shown for three different values of the mean molecular weight. The dashed curve is a (P,T) profile retrieved by inversion of IRIS thermal emission data (figure after Conrath et al. 1987).

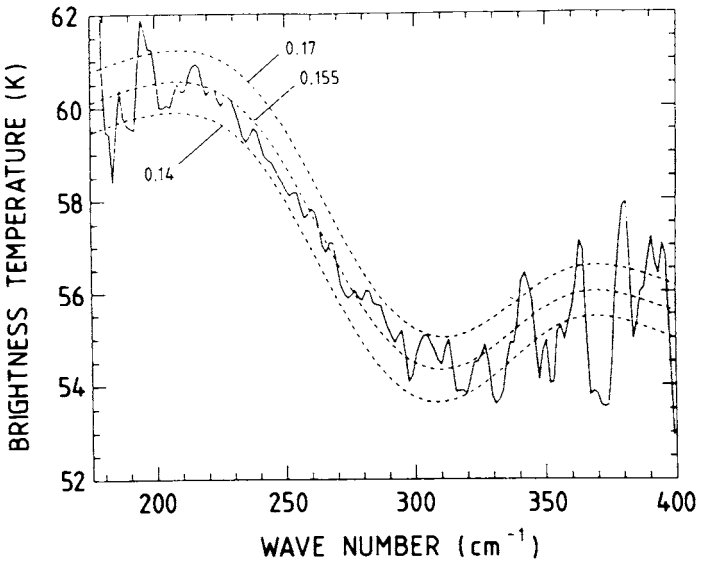

Fig. 4. A comparison of measured (solid curve) and calculated (dashed curve) thermal emission spectra. The solid curve is an average of 112 separate IRIS spectra. The three theoretical curves are calculated from the radio-occultation data for three different values of the helium mole fraction (figure after Conrath et al. 1987).

words, is the He/H_2 radial distribution uniform throughout the whole planet? The second question is whether we can infer the He/H_2 ratio of the primitive solar nebula from the Uranus value.

He/H_2 Radial Distribution in Uranus. At present, two mechanisms have been suggested for producing variations in the radial distribution of H_2 and He in the giant planets. One mechanism, that involves the fractionation of He from metallic hydrogen at the high pressures prevailing in the interiors of the giant planets, is discussed below. This mechanism is believed to be responsible for the different He abundances observed on Uranus and Saturn, and may also be operating on Jupiter, although the situation is less clear in this case. The second mechanism, originally proposed for Uranus by Stevenson (1984*b*) and Fegley and Prinn (1986), involves the differential solubilities of H_2 and He in the predicted water clouds in the lower troposphere of Uranus. This mechanism, which may be at least partially responsible for the apparently different He/H_2 ratios on Uranus and Neptune (Samuelson et al. 1989), is discussed later (Sec.IV.G).

A glimpse at Fig. 5 illustrates the first question: the observed He/H_2 value on Saturn appears to be substantially less than the Jupiter and Uranus values; the abundance in Jupiter may be depleted compared to Uranus, although the two results are marginally compatible. As the atmospheres of all the giant planets presumably were formed from the same hydrogen-helium

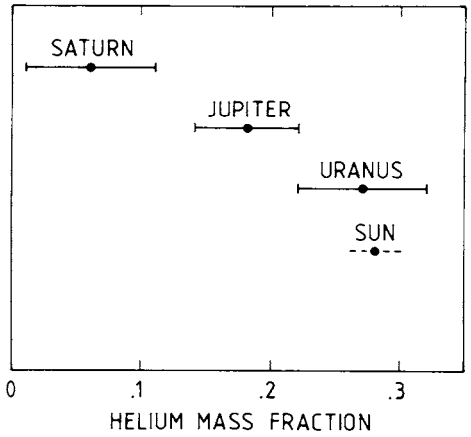

Fig. 5. A comparison of the helium abundance in solar system bodies with the value in the solar nebula. The latter value is derived from standard evolutionary models of the Sun (see Table I). Atmospheric values determined from Voyager measurements are given for the Jovian planets (figure after Conrath et al. 1987).

reservoir, namely the primitive solar nebula, one might expect them to exhibit similar abundances because the large masses and low exospheric temperatures of these objects preclude significant escape of even the lightest elements.

High pressure thermodynamics and theories of planetary evolution provide an interpretation of the observations. Figure 6 illustrates the behavior of a mixture of hydrogen and helium at temperatures and pressures occurring in the interiors of the giant planets. As long as hydrogen is in a molecular phase, helium is well mixed at expected planetary temperatures, within every giant planet. At pressures higher than about 3 Mbar (300 GPa), hydrogen becomes metallic (Nellis et al. 1983*b*). At sufficiently low temperature, helium is no longer miscible in H^+. Helium droplets form and migrate towards the center of the planet, leading to an enrichment of helium in the central part and to a depletion in the outer atmosphere.

Models of internal structure and of planetary evolution allow us to determine whether this process occurs in the interiors of the giant planets. The first point to consider is that Jupiter, Saturn and Neptune all exhibit internal sources of energy. It is generally assumed (although Stevenson [1985] has questioned the validity of this assumption) that the energy can be transferred only by convection (Hubbard 1984). Accordingly, the temperature-pressure profile within the planet is closely approximated by an adiabat. All planets have cooled continuously from the initial high temperature acquired during their formation (Stevenson 1982*a*,; Hubbard 1984*a*). The representative adiabats then move toward lower temperatures. As an example, Fig. 6 exhibits three Saturn adiabats corresponding to three different ages of the planet; the helium differentiation starts when the 3-Mbar pressure level reaches the sat-

uration temperature. As a matter of fact, helium solubilities in metallic hydrogen are uncertain, but the existence of an internal heat source in Jupiter and Saturn provides another constraint: evolutionary models of Saturn predict that the luminosity of this planet resulting from its accretion should have largely disappeared 1 or 2 Gyr ago (Graboske et al. 1975; Stevenson 1982*a*). The fact that Saturn still has an internal source of heat is thus consistent with the idea that helium droplets continuously migrate toward the center of the planet, thus liberating the gravitational energy responsible for the observed present luminosity.

The case of Jupiter is less clear owing to its greater mass and size. Its intrinsic luminosity is expected to vanish later than that of Saturn. Unfortunately, the uncertainty in the equation of state precludes a precise determination of the evolutionary time scale for Jupiter's interior.

A comparison of the observed He abundance in Jupiter with present estimates of the protosolar abundance, as discussed below, suggests that He differentiation has in fact already begun in Jupiter. That is also the opinion of Stevenson (1985) who, calibrating the He solubility curve from the observed depletion in Saturn compared to an assumed He abundance of 25% by mass in the solar nebula, predicted a He mass fraction of 18% in the outer atmosphere of Jupiter, in remarkable agreement with observations, although as Stevenson (1985) states, there is a large uncertainty in his estimated He mass fraction.

The case of Uranus, and probably of Neptune as well, is less simple than envisaged before the Voyager encounter. Previous interior models of both planets (Stevenson 1982*a;* Hubbard 1984*a;* Podolak and Reynolds 1984), constrained to fit the values of the J_2 and J_4 gravitational moments, assumed large cores compared to the size of the planet and relatively thin atmospheres. In these models, the H_2 pressure at the edge of the core did not exceed 200 Kbar, well below the value of the transition to a metallic state. Thus, no He differentiation was expected in the interior of Uranus (Fig.6).

Revised values of J_2 and especially of J_4, taking into account Voyager data, lead to a new view of the internal structure of this planet (Stevenson 1987; Hubbard and Marley 1989). Discrete layering is unlikely and hydrogen may be present in the deepest region, and thus possibly in a metallic phase. (For a more detailed discussion, see the chapter by Podolak et al.) However, the weakness of the observed internal source of energy, if any, of Uranus suggests that helium differentiation has not yet begun in Uranus or is still quite modest. Even if the initial luminosity of Uranus has completely vanished, the estimated amount of radioactive heating (Hubbard 1984) is sufficient to account for the internal heat flux ($\leq$ 1.14 times the absorbed solar flux) derived by Pearle et al. (1990). Furthermore, as discussed later in Sec. IV.G, the greater solubility of H_2 in water clouds in the lower troposphere of Uranus will increase the He/H_2 ratio by $\leq$ 2%, well within the uncertainties of the measured He/H_2 ratio. In other words, chemistry in the present-day

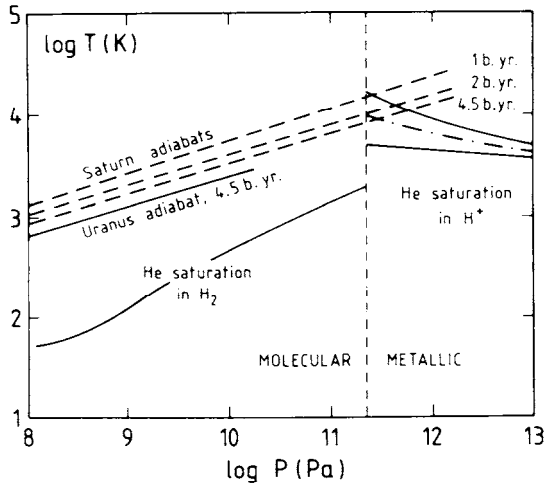

Fig. 6. Helium saturation in a "solar" composition (75% H by mass, 25% He by mass) mixture of hydrogen and helium is compared to several adiabatic (*P,T*) profiles for Saturn and Uranus. The vertical dashed line indicates the molecular to metallic phase transition for hydrogen. *Metallic region:* The two solid lines are theoretical estimates of the upper and lower limits to He solubility in H^+; the dash-dot line is taken as the most plausible value. The three different Saturn adiabats show estimated (*P,T*) profiles as the planet cools down and evolves to the present epoch (4.5 Gyr). The Saturn adiabats begin to intercept the most plausible solubility curve about 2 Gyr after the formation of the planet and helium raindrops form. *Molecular region:* The Saturn adiabats are always above the He solubility limit in H_2. The present-day Uranus adiabat is cooler than the Saturn adiabats, but is believed to stop at the edge of the planetary core ($P \sim 2 \times 10^{10}$ Pa) before reaching the metallic hydrogen region. The pressure is in pascals (1 bar = 10^5 Pa). (Figure is after Gautier and Owen [1989], who adapted the figure from Stevenson [1982a].)

atmosphere of Uranus will not dramatically alter the radial distribution of He and H_2. Thus it is very likely that the helium abundance measured in the atmosphere of Uranus is representative of the bulk He abundance of the planet. But, as questioned earlier, is this He abundance representative of the He abundance in the primitive solar nebula?

He/H_2 Variations During the Formation of Uranus. Whatever the scenario of formation of the giant planets (see Pollack and Bodenheimer 1989), H_2 and He initially must have been in the same ratio in their protoatmospheres as in the primitive solar nebula: physical conditions prevailing in the region of formation of these objects inhibited the condensation and fractionation of these gases. However, specific chemical processes could have modified the initial He/H_2 ratio in a way that depended on the composition of the nebula and on the formation processes of the giant planets. Inhomogeneous models of planetary formation (Perri and Cameron 1974; Mizuno 1980; Bodenheimer and Pollack 1986) assume that the cores were formed first from accretion of

planetesimals containing refractory materials as well as ices or clathrates made of CNO compounds. Subsequent accretional heating vaporizes the ices, forming a secondary atmosphere dominated by simple CNO compounds. As the growing planet accumulates an atmosphere of solar nebula gas, this envelope will be correspondingly enriched in carbon, nitrogen, oxygen and other heavy elements except neon, which was not captured by the core-forming ices (Gautier and Owen 1985,1989) because Ne ice and Ne clathrate cannot form in the solar nebula (Lewis 1972; Sill and Wilkening 1978). Another possibility initially advocated by Stevenson (1982*c*) and discussed in detail by Pollack et al. (1986*a*) is that infalling planetesimals enriched atmospheres in "heavy" elements after planetary formation.

In either case, the effect on the present atmospheric composition depends upon the composition of grains imbedded in the nebula. Fegley and Prinn (1986) and Prinn and Fegley (1989) proposed generic models for the composition of condensates that accreted to form Uranus, and their models can be used to illustrate the range of possibilities. At one extreme, the assumption of complete thermochemical equilibrium leads to condensates that contain CH_4 and NH_3 ices as well as NH_3 hydrate and CH_4 clathrate. In such a case, chemical reprocessing in the atmosphere of Uranus did not require hydrogen for producing CH_4 and NH_3, so that the reservoir of H_2 was not affected and the nebular He/H_2 ratio was preserved on Uranus.

If on the contrary Uranus was formed from a large reservoir of disequilibrium matter containing CO, CO_2, N_2 ices and clathrates and/or carbonaceous chondrite-like organic matter, the subsequent production of CH_4 and NH_3 within the protoatmosphere of the planet consumed hydrogen, leading to an increase of the He/H_2 ratio compared to the value in the solar nebula. In such a case, Prinn and Fegley (1989) predicted a maximum increase of 30% in the He abundance in Uranus. Fegley and Prinn (1986) showed that increases in the He/H_2 ratio depend upon the exact enrichment of carbon and nitrogen over their solar composition values. For example, if all carbon and nitrogen accreted by Uranus were in the form of CO and N_2, respectively, the observed carbon enrichment of $\sim$ 24 times solar (see Sec. III.B) implies an increase in the He/H_2 ratio of $\leq$ 10%. Pollack et al. (1986*a*) also predicted a He/H_2 enhancement but used a different approach: assuming that the carbon enrichment observed in all giant planets (see Sec. III.B.4) is caused by the dissolution of infalling planetesimals, they fit a semi-empirical model to the observed enrichment and derive an estimate of the fraction of carbon present in condensates imbedded in the nebula. Assuming in addition a carbonaceous chondrite-like composition for planetesimals—a questionable hypothesis considering the large diversity of nebula composition models proposed by Fegley and Prinn (1986) and the prevalence of ices in the region of formation of the giant planets—Pollack et al. (1986*a*) estimated an increase in the He/H_2 ratio in Uranus of 3 to 9% over the solar composition value. Thus, al-

though chemical processes during the accretion of Uranus may have increased the He/H_2 ratio over the solar value, the increases predicted for the observed carbon enrichment are $\sim$ 10%, which is within the uncertainty of the measured value on Uranus.

He/H_2 in the Sun and the Solar Nebula. The comparison of the observed He/H_2 ratio on Uranus to that in the solar nebula requires a precise estimate of the latter value. This information may be obtained from an inference of the He abundance in the early Sun. As mixing between the central region of the Sun and outer layers presumably has never occurred (see, e.g., Lebreton and Maeder 1987), observations of the He abundance in the solar atmosphere should provide the protosolar value.

Solar wind measurements are not helpful because various physical processes deplete the He abundance compared to the chromospheric value (Geiss 1982). Observations of helium lines in a prominence by Landman and Illing (1977) were analyzed by Heasley and Milkey (1978) who derived a per mass He abundance of $Y = 0.28 \pm 0.05$ (systematic errors are not considered). It is interesting to note that the central value of this determination is equal to the one derived by Pagel (1982), $Y = 0.28 \pm 0.02$, for the abundance of helium in the vicinity of the solar system (Orion nebula, normal stars). Results from surface oscillations are not yet conclusive. Gough (1983) announced from presently available data values of Y varying from 0.23 to 0.27, but the accuracy of the method is controversial: Guenther and Sarajedini (1988) have shown that p-mode frequencies are only very weakly sensitive to changes in the He abundance. On the other hand, Dappen and Gough (1986) claim that the inference of Y is possible by means of an inversion method applied to a large number of frequencies. However, it should be noted that the inversion method does not yield a single unique solution because a suite of density profiles (and thus of He abundances) can be fitted to the observations.

Therefore, at present, the most reliable method for inferring the protosolar He abundance makes use of evolutionary models that are fitted to the present mass, luminosity and age of the Sun. The best fit, which corresponds to the He protosolar abundance, depends on a number of input data, the most important of which are nuclear reaction cross sections, the equation of state, the elemental abundances and the radiative opacity. (For an extensive discussion, see Bahcall and Ulrich [1988].)

Improved radiative mean opacities calculated by Huebner et al. (1977) and updated nuclear data have recently become available. The solar abundances of heavy elements have also been re-evaluated (see, e.g., Grevesse 1984). Using these new data, five groups (see Table I) have independently derived He abundances in the range 0.27 to 0.28, while previous models led to $Y = 0.25$ (Bahcall et al. 1982). Standard models assume that elemental

TABLE I
Summary of Solar System and Primordial Helium Abundances

Determination	Y	References
	Uranus	
Voyager	0.262 ± 0.048	Conrath et al. 1987
	Saturn	
Voyager	0.06 ± 0.05	Conrath et al. 1984
	Jupiter	
Voyager	0.18 ± 0.04	Conrath et al. 1984
	Sun	
Cosmic rays	0.20 ± 0.04	Lambert 1967
Helium emission lines	0.28 ± 0.05	Heasley and Milkey 1978
Surface oscillations	$0.23 - 0.27$	Gough 1983
Evolutionary models	0.274	Vandenberg 1983
Evolutionary models	$0.274 - 0.282$	Noels et al. 1984
Evolutionary models	0.25	Bahcall et al. 1985
Evolutionary models	0.279	Lebreton and Maeder 1986
Evolutionary models	0.28	Cahen et al. 1986
Evolutionary models	0.276	Cahen 1986
	Solar Neighborhood	
Various objects, average	0.28 ± 0.02	Pagel 1982
	Primordial	
Extragalactic H II	$\leq 0.245 \pm 0.030$	Kunth 1981
Extragalactic H II	≤ 0.25	Davidson and Kinman 1985
Extragalactic H II	0.239 ± 0.015	Boesgaard and Steigman 1985
Extragalactic H II	0.207 ± 0.016	Ferland 1986
Extragalactic H II	0.24 ± 0.01	Kunth 1986
Extragalactic H II	0.232 ± 0.014	Shields 1987
Extragalactic H II	0.237 ± 0.005	Pagel 1986
Extragalactic H II	0.232 ± 0.004	Pagel 1987

abundances are the same at all points and at all times. In order to get a better fit to observed solar surface oscillations, nonstandard models have been elaborated (Bahcall and Ulrich 1988). These models assume that the initial helium abundance is larger in the interior than the outer region, but they lead to an increase of the discrepancy between the observed and calculated neutrino flux, and thus are less reliable than standard models. In any case, as stated above, the solar oscillations do not provide strong constraints on the He abundance.

The main difficulty is the inability of standard evolutionary models to explain the observed neutrino flux. Although predicted capture rates in the ^{37}Cl experiment have substantially decreased compared to old calculations (Bahcall and Ulrich 1988), the discrepancy between predictions and observations is still significant. Cahen et al. (1986) announced a capture rate of 6.4 ± 1.4 solar neutrino unit (SNU) and Bahcall and Ulrich (1988) reported 7.9 ± 2.6 SNU, while the rate observed from the ^{37}Cl experiment is 2.0 ± 0.3 SNU (Rowley et al. 1985). Bahcall and Ulrich (1988) discussed

extensively the neutrino problem, considering all sources of uncertainty. They showed that varying nuclear reaction rates up to the extreme values indicated by laboratory measurements can decrease the calculated neutrino flux somewhat, but not sufficiently to fit the observations. Incidentally, that also increases the helium abundance somewhat (Lebreton et al. 1988). The very complete analysis of Bahcall and Ulrich suggests that, unless nonphysical assumptions are introduced into the calculations, there is no way, at the present time, to solve the neutrino problem by means of evolutionary models.

On the other hand, a number of particle physics explanations have recently been proposed (e.g., weakly interacting massive particles, resonant neutrino oscillations, neutrino decay, neutrino electric or magnetic dipole moment, etc.). Several new solar neutrino experiments, involving ^{37}Cl, ^{71}Ga and ^{98}Mo detectors, are in progress and are expected to provide some light on neutrino physics, especially on the validity of the resonant neutrino oscillations theory (Mikheyev and Smirnov 1986).

If the solution of the problem is due to weak interaction physics, then the evolutionary models are valid and, unless the interior structure and the radiative opacity are changed drastically, it is likely that the presently inferred He abundance will not be substantially modified.

Thus, we assume that the He abundance in the primitive solar nebula was in the range 0.27 to 0.28 (by mass). For comparison, the He abundance (by mass) observed for Uranus is 0.262 ± 0.048, which, within the uncertainties, is the same as the value derived from standard evolutionary models of the Sun. This agreement indicates that the He/H_2 ratio observed on Uranus is probably representative of that in the primitive solar nebula. Finally, we also note that both the Uranus He abundance and the He abundance estimated from the standard evolutionary models are consistent with a "primordial" value of around 0.24 (Pagel 1987) because current models of chemical evolution of galaxies indicate an increase of ~ 0.03 in the He abundance due to production in stars between the origin of the universe and the origin of the solar system (Delbourgo Salvador et al. 1985).

He/H_2 on Neptune. The Voyager 2 encounter with Neptune in August 1989 provided an opportunity to determine the He/H_2 ratio by using the results of the IRIS (Conrath et al. 1989) and radio-occultation (Tyler et al. 1989) experiments as described earlier. Contrary to the cases of Jupiter, Saturn and Uranus, the data for Neptune indicate that opacity from a cloud or haze affects the far-infrared spectrum of the planet in the 200 to 400 cm^{-1} range (Samuelson et al. 1989). This makes the He abundance determination more difficult because it depends on the assumed model for the cloud and/or haze opacity. However, the preliminary analysis of Samuelson et al. (1989) suggests that the helium abundance is substantially *higher* than the value determined for Uranus. Should this result be confirmed, it has several possible interpretations. One interpretation is that the higher He abundance is due to

the consumption of H_2 during the accretion of Neptune. Another possible interpretation is that the higher He abundance is due to the differential solubility of He and H_2 in low-lying water clouds in the atmosphere of Neptune. However, the calculations of Fegley and Prinn (1986) for Uranus indicate that the enhancement of the He/H_2 ratio by this mechanism is only 2% for water cloud condensation at the critical point of 647 K. In either case, a higher He abundance on Neptune than on Uranus may be correlated with other differences such as the enrichment of carbon, nitrogen and oxygen over their solar abundances.

3. Hydrogen. Meanwhile, considerable progress has been made in studying the hydrogen abundance separately. The 4–0 quadrupole lines were discovered by Giver and Spinrad (1966), followed by the 3–0 lines (Lutz 1973), the 5–0 lines (Trafton 1978) and the 1–0 and 2–0 pressure-induced bands (Fink and Larson 1979). Owen et al. (1974) criticized the putative identification of the 4–0 pressure-induced band by Giver and Spinrad (1966), showing that a weak methane band occurred at the same wavelength and might account entirely or at least in part for the observed absorption of Uranus.

Belton et al. (1973) reported the first detection of Raman scattering on any planet, following a prediction by Wallace (1972). They found evidence for Stokes shifts in the reflected Fraunhofer spectrum around the H and K lines corresponding to the frequencies of both the S(0) and S(1) rotational transitions of H_2. They deduced that their observations required an H_2 column density of at least 200 km amagat.

Cochran and Trafton (1978) carried this work further, demonstrating that Raman and Rayleigh scattering models for the atmosphere of Uranus led to an ultraviolet albedo that was higher than the observed value, assuming a clear hydrogen atmosphere. They suggested that some kind of ultraviolet absorbing aerosol was present. Using the IUE to observe the spectrum of Uranus down to 2000 Å, Caldwell et al. (1981) found that the continuum matched Cochran's model in shape but was indeed too low at these wavelengths also. It now appears that the discrepancy is probably caused by a stratospheric aerosol (Pollack et al. 1987).

Direct determination of the H_2 column abundance from the intensities of the quadrupole lines was made difficult by problems with the definition of an appropriate line shape and the effects of particulate scattering in the atmosphere. Belton and Spinrad (1973) analyzed the $S_3(0)$ pressure-induced absorption on Uranus and found that here too, they had to introduce aerosols into their model atmosphere in order to achieve a high enough albedo to match the observations. McKellar (1974) demonstrated that previous workers had ignored the effects of pressure shifts on quadrupole lines, requiring reduction in the derived column abundances by about a factor of 2. Trafton (1976) carried out an extensive review of measurements of the 3–0 and 4–0

bands, which can now be augmented by his most recent work on the 3–0 band (Trafton 1987).

The consensus emerging from all of these studies is that one is seeing to a level in the Uranus atmosphere in the continuum or in weak absorption bands at wavelengths near 8000 Å that corresponds to a column abundance on the order of 250 ± 50 km amagat of H_2.

Smith (1978) called attention to the importance of accounting properly for the distribution of hydrogen between ortho ($J = 1, 3, 5, \ldots$) and para ($J = 0, 2, 4, \ldots$) states. In the ortho states, the spin axes of the two nuclei are aligned, in the para states they are anti-parallel. Ortho-para transitions are highly forbidden (e.g., see Farkas 1935 for a discussion). A *normal* distribution set at a high temperature in the planet's lower atmosphere should be perceived when the gas is brought by convection to the colder upper atmosphere. In *normal* hydrogen, the number of molecules in the ortho states is three times the number in the para states. In contrast, the lower temperature distribution is referred to as *equilibrium* hydrogen, where the population of different states is given by Boltzmann statistics. As Smith (1978) pointed out, there is an opportunity here to work back from the observed intensities of S(0) and S(1) quadrupole absorptions in the spectrum of Uranus (and the other giant planets) to deduce the ortho-para ratio and hence the thermal *history* of the hydrogen. The available observations suggested an equilibrium distribution, but both the quality of the observations and the difficulties in their interpretation prevented a firm conclusion from being reached.

Massie and Hunten (1982) discussed the ortho-para conversion problem in great detail, concluding that catalytic reactions with aerosol particles near the 1-bar level could convert ortho and para hydrogen. A significant deposition of energy in the aerosol layer might result owing to the difference in specific heat of the two forms of hydrogen (e.g., see Farkas 1935) which could have consequences for planetary dynamics. Gierasch (1983) pursued this possibility for Jupiter and Saturn, concluding that the effect could be important if the conversion times are of the same order as the dynamical time scales.

In the case of Uranus, the main problem with all of this is the possible stability of the deep atmosphere against convection. The lack of a strong internal heat source has been suggested to lead to a subadiabatic gradient at depths below the level where the temperature reaches about 220 K (de Pater and Massie 1985). Nevertheless, an adiabatic temperature gradient is expected as a consequence of the planetary accretion process (Lewis 1974*a;* but see Stevenson [1985] for a dissenting view) and is specifically assumed in interior structure models (e.g., see Hubbard 1984*a*). Thus it is presently uncertain if large amounts of disequilibrium hydrogen will appear in the upper troposphere. This conclusion is indeed consistent with the finding of Baines and Bergstralh (1986) that the fraction of equilibrium hydrogen in the visible atmosphere is $0.63 < f_e < 0.95$. Trafton (1987) finds $f_e = 0.75 \pm 0.10$.

4. The Ratio of Methane to Hydrogen. The idea that there probably is a higher relative abundance of methane to hydrogen in the atmospheres of Uranus and Neptune compared to Jupiter and Saturn probably goes back to the 1930s. It was already evident then that the methane absorptions were stronger on these more distant planets (see Sec. III.A) and it was well known that the densities of these two planets implied a higher proportion of heavy elements to hydrogen than existed on Jupiter and Saturn. Nevertheless, a rigorous test of this idea proved difficult.

Lutz et al. (1976), using McKellar's (1974) suggested correction of H_2 abundances, found that their study of methane suggested an overabundance of carbon to hydrogen ". . . by at least a factor of 20." If we use their published numbers (225 km amagat H_2, 5.8 km amagat CH_4), we find that the mole fraction of the atmosphere that is CH_4 is $0.016 < f_{CH_4} < 0.04$ or C/H = 27^{+15}_{-10} times the solar value of 4.7×10^{-4} (Lambert 1978).

In contrast, Fink and Larson (1979) found C/H = 2×10^{-3}, using their own values for the methane column abundance and a figure of 400 km amagat for H_2 derived by Danielson (1977). This corresponds to 4.3 times the solar value. They concluded that C/H is enriched over the solar value but not by much and shows remarkably little variation among the major planets.

This conclusion was endorsed by Trafton (1981), who found that "Present evidence suggests that the CH_4 mixing ratios for Uranus and Neptune probably fall in the range 1.3 to 6 times the solar abundance ratio." Teifel (1983) fitted both the methane bands and the intervening continuum of the visible spectrum of Uranus with a model atmosphere consisting of a high-altitude scattering haze layer above a semi-infinite Rayleigh scattering atmosphere. He found C/H = 1.5×10^{-3}, in agreement with Fink and Larson (1979).

The most comprehensive model atmosphere developed to date is probably that of Baines and Bergstralh (1986). They used the observations of a number of other investigators plus their own work on the geometric albedo spectrum and H_2 and CH_4 line profiles. They found that they could not accommodate Teifel's (1983) model (nor could Trafton [1987], working just with the 3–0 H_2 quadrupole lines). Instead, they developed a family of models with a haze layer above a clear region of the atmosphere which in turn has a semi-infinite opaque cloud as its lower boundary. Using the available observations to constrain the model parameters, they found a best fit for the pressure at the top of this cloud in the range of $2.4 < P_{cld} < 3.2$ bar corresponding to a column abundance of 250 to 315 km amagat of H_2 and a CH_4 mixing ratio of $0.020 < f_{CH_4} < 0.046$.

While the atmosphere of Uranus continues to pose problems in terms of the location and characteristics of haze and cloud layers (which may in fact be time variable [Lockwood et al. 1983]), at least a consensus has emerged among groundbased observers that C/H is enriched by more than a factor of

20 over the solar value. This was first established by Lutz et al. (1976) simply by using absorption bands of methane and hydrogen of comparable strength in a part of the spectrum where the continuum is well defined. In retrospect, this seems to be a satisfactory model-independent approach to the determination of mixing ratios. It also works well for the determination of D/H, as we shall see in Sec. III.B.5. Indeed, the deuterium evaluations support the conclusion from the methane studies that the atmospheres of Uranus and Neptune have very different compositions from those of Jupiter and Saturn.

5. Deuterium. In principle, the most straightforward way to determine D/H in the atmosphere of a giant planet is to evaluate abundances of HD and H_2. Unlike H_2, the HD molecule possesses a weak dipole moment because of the mass difference of the two nuclei. This asymmetry allows dipole transitions to occur, but the line strengths are very small. Nevertheless, the lines of the 4–0 band of HD have been reported in the spectrum of Uranus by several investigators who derived values or upper limits for D/H (see Trafton 1981). Combining their own observations with those of previous studies, Trafton and Ramsay (1980) obtained a value of $D/H = (4.8 \pm 1.5) \times 10^{-5}$. However, Smith et al. (1989) concluded from a meticulous study of the problem that in their opinion, ". . . no previously reported measurements have unequivocally detected an HD line in Uranus or Saturn . . .". They felt that the spectra in the vicinity of the HD lines are too contaminated by weak methane (or other hydrocarbon) absorptions to permit identification of the HD features. Instead, they suggested an upper limit of 10^{-4} for D/H on Uranus.

Hubbard and MacFarlane (1980*a*) predicted that D/H in the atmospheres of Uranus and Neptune should be enriched as a result of contributions of deuterium from hydrogen-bearing "ices" in the core of these two planets. Their idea was that the low temperature of the outer nebula would drive the isotopic equilibrium between hydrogen and the ice-forming compounds to near-terrestrial values of D/H in the ices. Unlike Jupiter and Saturn, Uranus and Neptune have core masses that are larger than 75% of the total planetary mass. Hence, materials coming from the cores can make a large difference in the composition of the atmosphere, as we saw in the previous discussion of the CH_4/H_2 ratio. However, the time required for the postulated isotopic exchange reaction to reach equilibrium is greater than the age of the solar system (see, e.g., Beer and Taylor 1973; Gautier and Owen 1985; Fegley and Prinn 1988*b*), and plausible catalysis mechanisms cannot overcome this kinetic inhibition (see, e.g., Grinspoon and Lewis 1987).

Nevertheless, this prediction was verified by the determination of D/H from observations of CH_3D and CH_4. The first attempt to find CH_3D on Uranus was made by Bardwell and Herzberg (1953) in the photographic infrared. They were unsuccessful, but set the stage for further efforts as longer

wavelengths became accessible. After identifying and analyzing the $3\nu_2$ band of CH_3D at 1.6 μm in the laboratory, Lutz et al. (1981) suggested that it might in fact be present in the spectra of Uranus and Titan previously published by Fink and Larson (1979). This suggestion was proved to be correct by de Bergh et al. (1986) who identified several features of the $3\nu_2$ band in a spectrum of Uranus recorded at a resolution of 1.2 cm^{-1}. They derived a value of D/H = $9^{+9.0}_{-4.5} \times 10^{-5}$. More recent work by de Bergh et al. (1990) has led to the detection of the $3\nu_2$ band of CH_3D on Neptune. The derived CH_3D/CH_4 ratio of $6^{+6}_{-4} \times 10^{-4}$ corresponds to D/H ~ $1.2^{+1.2}_{-0.8} \times 10^{-4}$, assuming equilibrium between CH_3D and HD and a fractionation factor of ~ 1.3 (de Bergh et al. 1990).

In contrast, values of this ratio determined from CH_3D observations in spectra of Jupiter and Saturn by a number of investigators led to D/H = $(2.6 \pm 1.0) \times 10^{-5}$ for Jupiter and D/H = $(1.7 \pm 1.0) \times 10^{-5}$ for Saturn (Fegley and Prinn 1988*b*); an average of D/H = $(2.0 \pm 1.5) \times 10^{-5}$ for both planets is given by Gautier and Owen (1989). This led Owen et al. (1986) to suggest that the outer solar system exhibited two distinct reservoirs of deuterium. The larger one must be the deuterium in gaseous hydrogen, corresponding to a value of D/H that existed in the original solar nebula and is still preserved in the atmospheres of Jupiter and Saturn where hydrogen dominates the other gases. The second, smaller reservoir consists of deuterium locked in the compounds that remained solid in the outer solar nebula and were thus unable to equilibrate with the hydrogen gas. This reservoir may actually contain several different values of D/H. Large enrichments of D/H compared with the current value of 1.5×10^{-5} in interstellar hydrogen (see, e.g., Geiss and Reeves 1981) are found among molecules detected in interstellar clouds. The idea is that such enhancements (produced by low-temperature ion-molecule reactions [see the review by Zinner 1988]) could at least partially be preserved during the process of solar system formation, provided the molecules were maintained at low temperature, isolated from the dominant hydrogen gas.

However, one must still exercise some caution about the CH_3D work, and these conclusions. The methane spectrum in the vicinity of the 1.6 μm CH_3D band is not rigorously understood. By ratioing CH_3D to CH_4 in the same part of the spectrum, using lines of similar strengths, the problems of line formation in the scattering atmosphere are minimized. In the case of Saturn, CH_3D bands at 8.7 μm, 5 μm and 1.6 μm all give similar values for D/H, suggesting that the method is rather robust (Gautier and Owen 1989). Still one would like to have independent evaluations of D/H on Uranus and Neptune to be absolutely certain of this result. One possibility for doing this is by observing the $R(0)$ and $R(1)$ lines of HD on Uranus and Neptune at submillimeter wavelengths (Bézard et al. 1986).

Taking the average value of D/H = $(2.0 \pm 1.5) \times 10^{-5}$ observed in the atmospheres of Jupiter and Saturn to be the value that existed in the solar

nebula may seem premature. For example, one might worry about possible isotopic fractionation in the planetary interiors, given the inferred precipitation of He in metallic hydrogen that is discussed in Sec. III.B.2. However, assuming that the transition from liquid molecular H_2 to liquid metallic hydrogen is first order, Hubbard (1974) calculated that deuterium will be enriched in the metallic hydrogen phase by $\leq 15\%$, which is well below the present uncertainties in the planetary D/H ratios. Also we note that Stevenson and Salpeter (1977) found that ". . . partitioning of deuterium between the various hydrogen-helium phases [in the interiors of these planets] appears to preserve the deuterium to hydrogen mass ratio, at least for $T \geq 5000$ K." They concluded that measurements of the D/H ratio in the outer convective envelopes of these planets would be representative of the bulk planetary D/H ratios.

The assumption that the Jovian and Saturnian average D/H ratio is representative of the D/H ratio in the solar nebula is apparently substantiated by the recent re-determination of the protosolar D/H ratio by Anders and Grevesse (1989) who give D/H $= (3.4 \pm 1.0) \times 10^{-5}$. Using a procedure developed by Black (1972) and Geiss and Reeves (1972,1981), Anders and Grevesse determined the difference between the $^3He/^4He$ ratios in "solar" and "planetary" gas components in meteorites. This yields the amount of ^3He produced by deuterium burning in the Sun, and hence the primordial deuterium abundance and D/H ratio. Given the uncertainties in both methods, the agreement between the Jupiter-Saturn value and the meteoritic value seems satisfactory. It will clearly be very interesting to see what value of D/H is observed by the Galileo Jupiter probe, which will make the first *in situ* measurement of deuterium in any of the giant planets.

6. Upper Limits on Minor Constituents. Several gases have been sought in the atmosphere with no success. A collection of current upper limits is given in Table II. Fink and Larson (1979) looked specifically for those gases that have absorption bands in the relatively clear regions of the spectrum between the strong methane bands. They selected gases for which laboratory spectra were available, either their own or those of other investigators. The unpublished limit on CO by de Bergh et al. (1985) is based on an analysis of the spectrum of Uranus at the time these authors discovered CO on Titan (Lutz et al. 1983) and CH_3D on Uranus (de Bergh et al. 1986). This is therefore a preliminary value that requires refinement. The CO limit from Caldwell et al. (1981) is based on the absence of the Cameron bands in the near ultraviolet in IUE spectra of the planet.

7. Voyager Results. One hoped that the Voyager encounter with Uranus would resolve the ambiguities left in the interpretation of groundbased observations and produce a definitive model for the Uranus atmosphere. Although the data set acquired by the various Voyager instruments was not quite

wavelengths became accessible. After identifying and analyzing the $3\nu_2$ band of CH_3D at 1.6 μm in the laboratory, Lutz et al. (1981) suggested that it might in fact be present in the spectra of Uranus and Titan previously published by Fink and Larson (1979). This suggestion was proved to be correct by de Bergh et al. (1986) who identified several features of the $3\nu_2$ band in a spectrum of Uranus recorded at a resolution of 1.2 cm^{-1}. They derived a value of D/H = $9^{+9.0}_{-4.5} \times 10^{-5}$. More recent work by de Bergh et al. (1990) has led to the detection of the $3\nu_2$ band of CH_3D on Neptune. The derived CH_3D/CH_4 ratio of $6^{+6}_{-4} \times 10^{-4}$ corresponds to D/H ~ $1.2^{+1.2}_{-0.8} \times 10^{-4}$, assuming equilibrium between CH_3D and HD and a fractionation factor of ~ 1.3 (de Bergh et al. 1990).

In contrast, values of this ratio determined from CH_3D observations in spectra of Jupiter and Saturn by a number of investigators led to D/H = $(2.6 \pm 1.0) \times 10^{-5}$ for Jupiter and D/H = $(1.7 \pm 1.0) \times 10^{-5}$ for Saturn (Fegley and Prinn 1988*b*); an average of D/H = $(2.0 \pm 1.5) \times 10^{-5}$ for both planets is given by Gautier and Owen (1989). This led Owen et al. (1986) to suggest that the outer solar system exhibited two distinct reservoirs of deuterium. The larger one must be the deuterium in gaseous hydrogen, corresponding to a value of D/H that existed in the original solar nebula and is still preserved in the atmospheres of Jupiter and Saturn where hydrogen dominates the other gases. The second, smaller reservoir consists of deuterium locked in the compounds that remained solid in the outer solar nebula and were thus unable to equilibrate with the hydrogen gas. This reservoir may actually contain several different values of D/H. Large enrichments of D/H compared with the current value of 1.5×10^{-5} in interstellar hydrogen (see, e.g., Geiss and Reeves 1981) are found among molecules detected in interstellar clouds. The idea is that such enhancements (produced by low-temperature ion-molecule reactions [see the review by Zinner 1988]) could at least partially be preserved during the process of solar system formation, provided the molecules were maintained at low temperature, isolated from the dominant hydrogen gas.

However, one must still exercise some caution about the CH_3D work, and these conclusions. The methane spectrum in the vicinity of the 1.6 μm CH_3D band is not rigorously understood. By ratioing CH_3D to CH_4 in the same part of the spectrum, using lines of similar strengths, the problems of line formation in the scattering atmosphere are minimized. In the case of Saturn, CH_3D bands at 8.7 μm, 5 μm and 1.6 μm all give similar values for D/H, suggesting that the method is rather robust (Gautier and Owen 1989). Still one would like to have independent evaluations of D/H on Uranus and Neptune to be absolutely certain of this result. One possibility for doing this is by observing the $R(0)$ and $R(1)$ lines of HD on Uranus and Neptune at submillimeter wavelengths (Bézard et al. 1986).

Taking the average value of D/H = $(2.0 \pm 1.5) \times 10^{-5}$ observed in the atmospheres of Jupiter and Saturn to be the value that existed in the solar

nebula may seem premature. For example, one might worry about possible isotopic fractionation in the planetary interiors, given the inferred precipitation of He in metallic hydrogen that is discussed in Sec. III.B.2. However, assuming that the transition from liquid molecular H_2 to liquid metallic hydrogen is first order, Hubbard (1974) calculated that deuterium will be enriched in the metallic hydrogen phase by $\leq 15\%$, which is well below the present uncertainties in the planetary D/H ratios. Also we note that Stevenson and Salpeter (1977) found that ". . . partitioning of deuterium between the various hydrogen-helium phases [in the interiors of these planets] appears to preserve the deuterium to hydrogen mass ratio, at least for $T \geq 5000$ K." They concluded that measurements of the D/H ratio in the outer convective envelopes of these planets would be representative of the bulk planetary D/H ratios.

The assumption that the Jovian and Saturnian average D/H ratio is representative of the D/H ratio in the solar nebula is apparently substantiated by the recent re-determination of the protosolar D/H ratio by Anders and Grevesse (1989) who give D/H $= (3.4 \pm 1.0) \times 10^{-5}$. Using a procedure developed by Black (1972) and Geiss and Reeves (1972,1981), Anders and Grevesse determined the difference between the $^3He/^4He$ ratios in "solar" and "planetary" gas components in meteorites. This yields the amount of ^3He produced by deuterium burning in the Sun, and hence the primordial deuterium abundance and D/H ratio. Given the uncertainties in both methods, the agreement between the Jupiter-Saturn value and the meteoritic value seems satisfactory. It will clearly be very interesting to see what value of D/H is observed by the Galileo Jupiter probe, which will make the first *in situ* measurement of deuterium in any of the giant planets.

6. Upper Limits on Minor Constituents. Several gases have been sought in the atmosphere with no success. A collection of current upper limits is given in Table II. Fink and Larson (1979) looked specifically for those gases that have absorption bands in the relatively clear regions of the spectrum between the strong methane bands. They selected gases for which laboratory spectra were available, either their own or those of other investigators. The unpublished limit on CO by de Bergh et al. (1985) is based on an analysis of the spectrum of Uranus at the time these authors discovered CO on Titan (Lutz et al. 1983) and CH_3D on Uranus (de Bergh et al. 1986). This is therefore a preliminary value that requires refinement. The CO limit from Caldwell et al. (1981) is based on the absence of the Cameron bands in the near ultraviolet in IUE spectra of the planet.

7. Voyager Results. One hoped that the Voyager encounter with Uranus would resolve the ambiguities left in the interpretation of groundbased observations and produce a definitive model for the Uranus atmosphere: Although the data set acquired by the various Voyager instruments was not quite

TABLE II
Near-Infrared and Ultraviolet Upper Limits on Minor Constituents

Molecule	Column Abundance[a] (cm am)	Volume Mixing Ratio[b]	Reference
NH_3	5	1.6×10^{-7}	Fink & Larson 1979
H_2S	30	1.0×10^{-6}	
C_2H_4	20	6.7×10^{-7}	
CH_3NH_2	10	3.3×10^{-7}	
CO	—	2×10^{-4}	Caldwell et al. 1981
CO	—	1×10^{-6}	de Bergh et al. 1985

[a]A column abundance of one centimeter amagat (cm am) is equivalent to 2.68×10^{19} molecules cm^{-2}.
[b]Using 300 km am H_2

up to this goal, at least some significant advances were made, especially by the radio-occultation experiment (Lindal et al. 1987).

To make the radio-occultation temperature profiles agree with the infrared temperature data, Lindal et al. (1987) found a mean molecular mass of 2.31 ± 0.06 amu. This gives an upper limit for the helium mixing ratio of $15.2 \pm 3.3\%$ by number, assuming the remainder to be hydrogen. In fact, above the water-cloud condensation level, one anticipates the next most abundant gas after helium to be methane, since neon should not be enriched over the solar value relative to hydrogen (Ne/H $\sim 10^{-4}$) because Ne ice and Ne clathrate do not condense in the solar nebula (Lewis 1972; Sill and Wilkening 1978; Gautier and Owen 1989). Even if nitrogen is enriched in the same proportion as carbon and all of it is present as N_2, the CH_4/N_2 ratio is still ~ 6.

A methane cloud layer at the 1.2-bar level with a thickness of 2 to 4 km was deduced from the refractivity data. This corresponds to the bottom of the upper haze layer in the standard model of Baines and Bergstralh (1986). Below this cloud layer, the methane mixing ratio was taken to be constant and independent of altitude. The adiabatic lapse rate was computed for equilibrium hydrogen, under the assumption that the rates of conversion of ortho to para H_2 states are too slow to have an appreciable effect on the temperature lapse rate (see Sec. III.B). Under these conditions, the nominal model of Lindal et al. (1987) led to a methane mole fraction of 2.3% below the clouds. This corresponds to an enrichment of C/H over the solar value by a factor of 24, in good agreement with Lutz et al. (1976) and Baines and Bergstralh (1986).

The lower bound of the radio occultation data was 2.3 bar, just above the highest level for the semi-infinite cloud layer deduced by Baines and Bergstralh (1986) at 2.4 bar, corresponding to 240 km amagat of H_2, in good agreement with other groundbased work (see Secs. III.B.3 and III.B.4).

The stratospheric haze that was visible in enhanced Voyager images (Smith et al. 1986) was studied in detail by Pollack et al. (1987). These authors favored a model that had the haze concentrated near 44 mbar with particles characterized by a model radius and number density of 0.13 ± 0.02 μm and 2 ± 1 particles cm^{-3}, respectively. They suggested that the main source of the aerosols is the condensation of photochemically produced hydrocarbons, such as ethane, acetylene and diacetylene. Solar ultraviolet irradiation of these ices can then produce polymers that absorb in the visible and ultraviolet. These could be the source of the absorbing haze required by Trafton (1987) to interpret his observations of the 3–0 H_2 quadrupole lines although Trafton specified 150 mbar as the lower bound of his haze layer. Further analysis might reconcile these two results. The possibility of temporal variations can be tested by future groundbased observations of the H_2 lines.

One concludes that the general picture being drawn from the Earth-based observations regarding the methane mole fraction, the ortho-para ratio of H_2, and the vertical structure of the atmosphere is consistent with the Voyager occultation results. The high enrichment of methane in particular now seems well established.

IV. CHEMICAL MODELS

A. Carbon

The spectroscopic observations reviewed in Sec. III indicate that CH_4 is the dominant carbon-bearing gas in the atmosphere of Uranus. Furthermore, the spectroscopic upper limit of $\sim 10^{-6}$ on the CO mixing ratio (de Bergh et al. 1985) combined with the CH_4 mixing ratio of 2.3% inferred from the Voyager 2 radio occultation experiment (Lindal et al. 1987) demands that the CH_4/CO ratio in the observable region of the atmosphere is at least 23,000 and may be even larger. This situation is in distinct contrast to the predicted CH_4/CO ratio of $\sim 10^{-7}$ for the solar nebula out of which Uranus formed (Fegley and Prinn 1989).

The reasons for the dominance of CH_4 over CO in the atmosphere of Uranus (as well as in the atmospheres of the other giant planets) can be easily understood by considering the net thermochemical reaction

$$CO(g) + 3H_2(g) = CH_4(g) + H_2O(g) \quad (1)$$

which interconverts the two gases. The equilibrium constant (K_1) for Reaction (1) is given by

$$K_1 = f_{CH_4} \cdot f_{H_2O}/(f_{H_2}^3 \cdot f_{CO}) \quad (2)$$

where f_i is the fugacity of species i and is related to the partial pressure (p_i) via a multiplicative factor ϕ_i known as the fugacity coefficient. Fugacity coefficients are unity for ideal gases and may be either greater than or less than unity for real gases. They are useful because they allow us to model the thermochemical equilibria of real gases, such as in the deep atmosphere of Uranus, by using tables of thermodynamic data for ideal gases (e.g., the JANAF Tables) combined with fugacity coefficients estimated from the theory of corresponding states (e.g., as described by Hirschfelder et al. [1954] and Prausnitz et al. [1986]).

The equilibrium constant expression can then be rewritten as

$$K_1 = [X_{CH_4} \cdot X_{H_2O}/(X_{H_2}^3 \cdot X_{CO})] \cdot [\phi_{CH_4} \cdot \phi_{H_2O}/(\phi_{H_2}^3 \cdot \phi_{CO})] \cdot P_T^{-2} \quad (3)$$

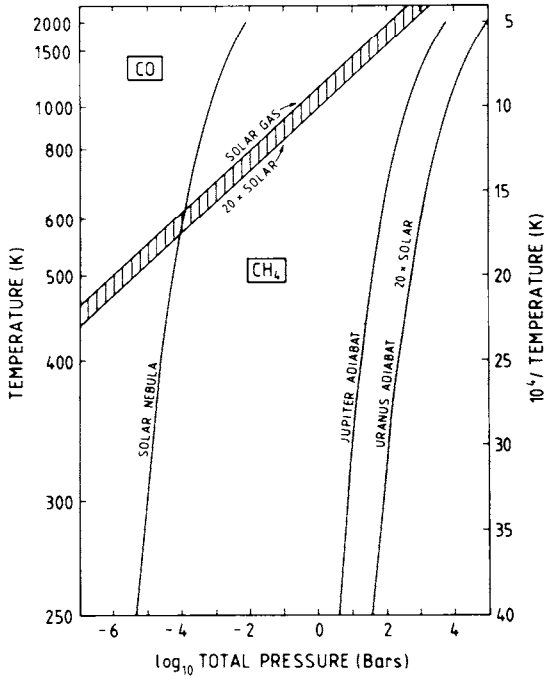

Fig. 7. The chemical equilibrium distribution of carbon between CH_4 and CO in solar composition gas as a function of temperature and pressure. Model (P,T) profiles for the solar nebula (Fegley and Prinn 1989), the Jovian atmosphere (Fegley and Prinn 1988*b*), and the Uranian atmosphere are shown in relation to the boundary between CH_4-rich and CO-rich regions. The upper side of the shaded boundary is the line where CH_4 and CO have equal abundances in solar composition gas. The lower side of the shaded boundary shows where CH_4 and CO have equal abundances in a gas enriched in all elements heavier than He by 20 times solar. Nonideality will shift the CH_4 – CO boundary toward the left, thus decreasing the CO/CH_4 ratio at a given temperature in the atmosphere of Uranus (figure modified from Fegley 1988*b*).

to show explicitly the dependence on the total pressure (P_T) and on the individual mixing ratios (X_i). Some further rearranging finally yields the equation

$$P_T = [\Phi_1 \cdot (X_{H_2O}/X_{H_2}^3) \cdot K_1^{-1}]^{1/2} \quad (4)$$

when $X_{CH_4} = X_{CO}$ and where $\Phi_1 = [\phi_{CH_4} \cdot \phi_{H_2O}/(\phi_{H_2}^3 \cdot \phi_{CO})]$ is the fugacity coefficient quotient in Eq. (3). Because the equilibrium constant K_1 is temperature dependent, Eq. (4) describes the position in (P, T) space of the line where CO and CH_4 have equal abundances.

An ideal gas (i.e., assuming $\Phi_1 = 1.0$) chemical equilibrium calculation of the CO − CH_4 boundary is illustrated in Fig. 7 for the case of a solar composition gas and also for the case of a gas enriched by 20 times the solar abundances in all elements heavier than He. Several important points are illustrated by this figure. First, the (P,T) profiles of the atmospheres of the giant planets are well to the right of the CO − CH_4 boundary in the CH_4-dominated region. In contrast, the (P,T) profile for the solar nebula is well inside the CO-dominated region at high temperatures. Although the solar nebula (P,T) profile crosses into the CH_4-rich region at lower temperatures, the CO to CH_4 conversion is kinetically inhibited at these low densities and temperatures and does not occur over the lifetime of the solar nebula (e.g., see the recent discussion by Fegley and Prinn [1989]). Thus, the formation of Uranus, either directly from the solar nebula or via an intermediate subnebula, involves the conversion of CO to CH_4.

Second, as we move along the planetary adiabats deeper into the atmospheres of Uranus and the other giant planets, we move closer to the CO − CH_4 boundary and thus move into atmospheric regions with larger amounts of CO. This is illustrated in Fig. 8 where the calculated CO/CH_4 ratio in the atmosphere of Uranus is compared to the observational upper limit. The predicted CO/CH_4 ratio, which is for the 20 times solar Uranus atmospheric model shown in Fig. 7, is computed from the equilibrium constant expression for Reaction (1)

$$(X_{CO}/X_{CH_4}) = (X_{H_2O}/X_{H_2}^3) \cdot \Phi_1 \cdot K_1^{-1} \cdot P_T^{-2} \quad (5)$$

taking K_1 from the JANAF Tables, the total pressure P_T from the atmospheric model, and $\Phi_1 = 1.0$. Fegley and Prinn (1986) showed that $\Phi_1 \sim 0.1$ at $\sim$ 900 K for their 500 times solar Uranus model atmosphere. Thus the expected nonideality of gases in the deep atmosphere of Uranus will reduce the predicted (CO/CH_4) ratio at a given temperature. However, this behavior will only serve to reinforce the conclusions derived from the present treatment.

Figure 8 shows that the observational upper limit of (CO/CH_4) $\sim 4.4 \times 10^{-5}$ corresponds to the CO/CH_4 ratio at $\sim$ 1700 K in the deep atmosphere

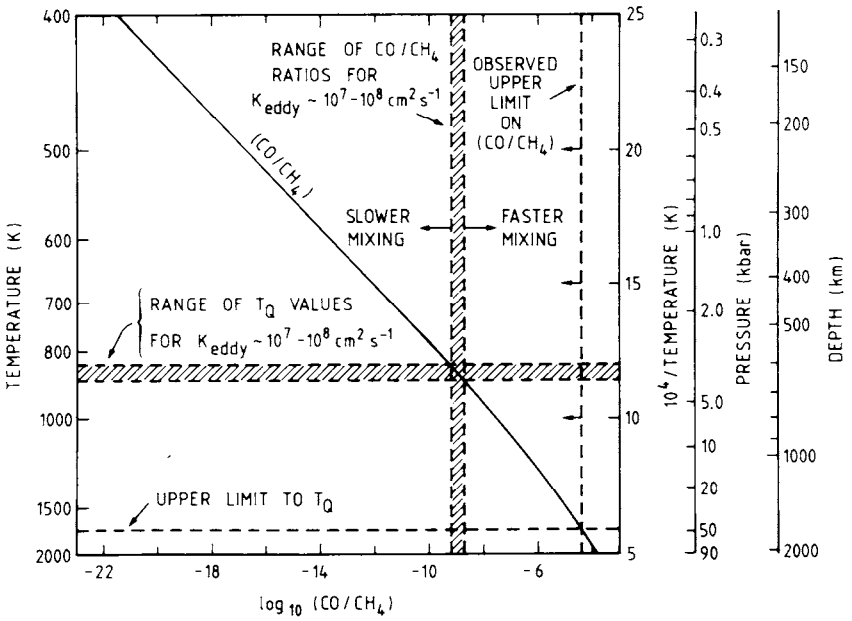

Fig. 8. The calculated CO/CH_4 ratio in the atmosphere of Uranus is compared to the observational upper limit. The ideal gas chemical equilibrium calculations are for the 20 times solar Uranus adiabat shown in Fig. 7. The vertical scales indicate temperature, pressure (dry lapse rate), and depth (below the 300 K level) along this model adiabat. The vertical and horizontal shaded bands are predicted CO/CH_4 ratios and quench temperatures calculated as described by Fegley and Prinn (1985*a*). The chosen vertical eddy diffusion coefficients $K_{eddy} = 10^7$ to 10^8 cm^2 s^{-1} are appropriate for assumed convective heat fluxes of 10 to 100 erg cm^{-2} s^{-1} (Danielson 1977; Hubbard 1978). The observational upper limit on the CO/CH_4 ratio corresponds to a much higher quench temperature and thus to much more rapid vertical mixing. Nonideality will shift the calculated curve to the left thus giving smaller CO/CH_4 ratios at each temperature (figure after Fegley 1990*a*).

of Uranus. Assuming that vertical mixing from deeper regions is the only possible source of CO, 1700 K is then the upper limit to the CO quench temperature (T_Q) on Uranus. At higher temperatures (i.e., deeper in the atmosphere), CO and CH_4 are rapidly interconverted, chemical equilibrium prevails and larger (CO/CH_4) ratios are produced. However, at lower temperatures (i.e., higher up in the atmosphere), chemical reaction rates are slower, CO and CH_4 are not as rapidly interconverted, and the equilibrium CO/CH_4 ratios are smaller. However, depending on the rate of vertical mixing there may be insufficient time to interconvert CO and CH_4 before an air parcel is convected upward.

Mathematically, for $T > T_Q$, the chemical lifetime (t_{chem}) for CO is less than the convective mixing time (t_{conv}). However, for $T < T_Q$ the reverse inequality (i.e., $t_{chem} > t_{conv}$) holds, while at the quench temperature $t_{chem} = t_{conv}$ is true. In the present case, calculating t_{chem} from the relevant

kinetic data (e.g., see Fegley and Prinn 1985*a* for a detailed explanation) yields $t_{chem} = t_{conv} \sim 10^{-2.8}$ s at 1700 K for the 20 times solar Uranus atmosphere model. The corresponding vertical eddy diffusion coefficient K_{eddy} is given by

$$K_{eddy} \sim H^2 / t_{conv} \tag{6}$$

where H is the pressure scale height. Inserting the appropriate numbers yields $K_{eddy} \sim 2 \times 10^{18}$ cm^2 s^{-1} for $T_Q \sim 1700$ K.

Unfortunately, the derived K_{eddy} value is not a useful upper limit on vertical mixing in the deep atmosphere of Uranus because it corresponds to physically impossible vertical mixing velocities and internal heat fluxes. For example, the vertical velocity $w \sim K/H \sim 4 \times 10^{10}$ cm s^{-1}, or about 10^5 times the sound speed in solar composition gas at the same temperature. Likewise, the simple relationship

$$K_{eddy} \sim H(\phi/\rho\gamma)^{1/3} \tag{7}$$

between the K_{eddy} coefficient, the scale height, the heat flux ϕ, the density ρ and $\gamma = C_p/R$ for free convection in a nonrotating system (e.g., see Stone 1976) implies $\phi \sim 10^{32}$ erg cm^{-2} s^{-1} when the values appropriate to the 1700 K level of our atmosphere model are inserted into Eq. (7).

More realistic K_{eddy} values, which are calculated from Eq. (7) by taking estimated heat fluxes of 10 to 100 erg cm^{-2} s^{-1}, are in the range of $\sim 5 \times 10^7$ to 10^8 cm^2 s^{-1}. The lower heat flux of $\sim$ 10 erg cm^{-2} s^{-1} is Danielson's (1977) estimate of radioactive heating from chondritic material in the core of Uranus, and the upper heat flux of $\sim$ 100 erg cm^{-2} s^{-1} is Hubbard's (1978) estimate of remaining primordial heat escaping from Uranus. As discussed by Allison et al. in their chapter, the recent analysis of Voyager IRIS measurements by Pearl et al. (1990) implies that the most probable value for the internal heat flux is $\sim$ 42 erg cm^{-2} s^{-1}. This value is about 4 times larger than Danielson's (1977) estimate and corresponds to $K_{eddy} \sim 7.6 \times 10^7$ cm^2 s^{-1} from Eq. (7). As noted by Fegley and Prinn (1986), the K_{eddy} values estimated from Eq. (7) imply slower vertical mixing on Uranus than on Jupiter or Saturn where K_{eddy} values of 10^8 to 10^9 cm^2 s^{-1} appear appropriate for the deep atmospheres (Flasar and Gierasch 1977; Stone 1976; Fegley and Prinn 1985*a*).

As Fig. 8 illustrates, K_{eddy} values of $\sim 10^7$ to 10^8 cm^2 s^{-1} correspond to quench temperatures of $\sim$ 830 to 880 K and to (CO/CH_4) ratios of about $10^{-9.2}$ to $10^{-8.7}$. However, even though the present observational upper limit on the CO/CH_4 ratio is about 20,000 to 60,000 times larger than the predicted value, the steep dependence of the CO/CH_4 ratio on temperature (and thus on mixing rate) displayed in Fig. 8 means that this ratio is potentially a very good spectroscopic probe of conditions in the deep, otherwise unobservable

regions of the atmosphere of Uranus. We also note that the (CO/CH_4) ratio provides a constraint on the H_2O abundance in the deep atmosphere of Uranus (see Fegley and Prinn [1988*a*] for a discussion of a similar constraint on the Jovian water abundance). Therefore it is important to make more sensitive observations designed to detect CO on Uranus. For example, observations in the submillimeter region might detect CO on Uranus (Bézard et al. 1986).

Finally, we can consider the thermochemical equilibria responsible for the production of higher hydrocarbons from methane. These are exemplified by the reactions

$$2CH_4(g) = C_2H_6(g) + H_2(g) \quad (8)$$

$$2CH_4(g) = C_2H_4(g) + 2H_2(g) \quad (9)$$

$$2CH_4(g) = C_2H_2(g) + 3H_2(g). \quad (10)$$

Rearranging the equilibrium constant expressions for Reactions (8) through (10) then yields the equilibrium mixing ratios for C_2H_6, C_2H_4 and C_2H_2

$$X_{C_2H_6} = K_8 \cdot (X^2_{CH_4}/X_{H_2}) \cdot \phi^2_{CH_4}/(\phi_{C_2H_6} \cdot \phi_{H_2}) \quad (11)$$

$$X_{C_2H_4} = K_9 \cdot (X^2_{CH_4}/X^2_{H_2}) \cdot \phi^2_{CH_4}/(\phi_{C_2H_4} \cdot \phi^2_{H_2}) \cdot P_T^{-1} \quad (12)$$

$$X_{C_2H_2} = K_{10} \cdot (X^2_{CH_4}/X^3_{H_2}) \cdot \phi^2_{CH_4}/(\phi_{C_2H_2} \cdot \phi^3_{H_2}) \cdot P_T^{-2}. \quad (13)$$

Figure 9 shows the temperature dependence of these mixing ratios. As discussed in the chapter by Atreya et al. C_2H_2 has been observed in the stratosphere of Uranus at a mixing ratio of $\sim 10^{-8}$ and IRTF measurements by Orton et al. (1987*b*) place an upper limit of 2×10^{-8} on the C_2H_6 mixing ratio. The results in Fig. 9 show that comparable mixing ratios for C_2H_2 in chemical equilibrium with CH_4 are not attained until temperatures greater than 2000 K, over 2000 km beneath the Uranian stratosphere. Thus a deep atmospheric contribution to the observed C_2H_2 abundance is not expected. However, it is interesting to note that the ideal gas calculations shown in Fig. 9 suggest a substantial C_2H_6 abundance ($\sim$ 0.04 ppm) in the Uranian troposphere if C_2H_6 destruction is quenched at temperatures around 1000 K, as Lewis and Fegley (1984) estimated for Jupiter.

B. Nitrogen

Although nitrogen is the fourth most abundant chemically reactive element (after H, O and C) in solar composition material (Cameron 1982) and NH_3 is the second most abundant spectroscopically active gas in the atmospheres of Jupiter and Saturn, no nitrogen-bearing compounds have been detected to date on Uranus. In fact, the inferred ammonia depletion in the 150 to 200 K region of the atmosphere by 100 to 200 times relative to the solar NH_3/H_2 mixing ratio (de Pater and Massie 1985; de Pater and Gulkis 1988; Gulkis et al. 1978,1983; Klein and Turegano 1978; de Pater et al. 1989;

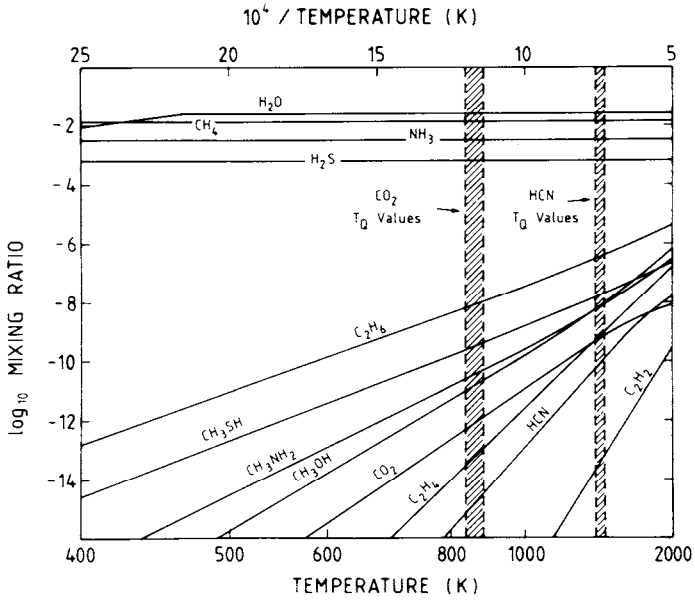

Fig. 9. Ideal gas thermodynamic equilibrium abundances of important H, C, N, O, S-bearing gases along the 20 times solar Uranus adiabat shown in Fig. 7. Volume mixing ratios are plotted as a function of inverse temperature. The CO/CH_4 and N_2/NH_3 ratios are shown separately in Figs. 8 and 11, respectively. The two vertical shaded regions show the range of calculated quench temperatures (T_Q) appropriate for K_{eddy} values of 10^7 to 10^8 cm^2 s^{-1}. The corresponding mixing ratios at T_Q for CO_2 and HCN are given in Table III. Other potential chemical probes of the Uranian deep atmosphere are C_2H_6, CH_3SH, CH_3NH_2, CH_3OH, C_2H_4 and C_2H_2. Note that $T_Q \sim 1000$ K will give mixing ratios of $\sim 4 \times 10^{-8}$ for C_2H_6 and $\sim 10^{-10}$ to $\sim 10^{-9}$ for CH_3SH, CH_3NH_2 and CH_3OH. Observations of several of these species may be possible with a suitably designed mass spectrometer on an entry probe (figure after Fegley 1900*a*).

Hofstadter and Muhleman 1989), is one of the major unresolved issues about the chemistry of the atmosphere of Uranus.

Despite the failure to detect ammonia, chemical thermodynamic principles demonstrate that NH_3 should be the dominant nitrogen-bearing gas in the atmosphere of Uranus. The chemical reaction

$$N_2(g) + 3H_2(g) = 2NH_3(g) \tag{14}$$

which interconverts N_2 and NH_3, has an equilibrium constant K_{14} given by

$$K_{14} = [X^2_{NH_3}/(X_{N_2} \cdot X^3_{H_2})] \cdot [\phi^2_{NH_3}/(\phi_{N_2} \cdot \phi^3_{H_2})] \cdot P_T^{-2}. \tag{15}$$

Rearranging Eq. (15) and setting $X_{NH_3} = X_{N_2}$ allows us to calculate the line in (P,T) space where N_2 and NH_3 have equal abundances. The results of an

ideal gas calculation of the $N_2 - NH_3$ boundary in solar composition gas and in a gas enriched in all elements heavier than He by 20 times solar are shown in Fig. 10.

Again it is clear that the (*P,T*) profiles for the atmospheres of the gas giant planets are well inside the NH_3 dominated field while the exemplary (*P,T*) profile for the solar nebula is well inside the N_2-dominated region until low temperatures where the N_2 to NH_3 conversion is kinetically inhibited (e.g., see Norris 1980). However, conversion between these two species is orders of magnitude faster in the hot, high pressure environments present in the deep atmospheres of the gas giant planets. As Fig. 11 illustrates, K_{eddy} values of 10^7 to 10^8 cm^2 s^{-1} allow Reaction (14) to proceed down to temperatures of about 1500 K where quenching occurs. The resulting (N_2/NH_3) ratio of $\sim 10^{-2.8}$ corresponds to a predicted N_2 mixing ratio of about 4 ppm. Several authors (see, e.g., Fegley and Prinn 1985*b*, 1986; Stevenson 1984*b*) have

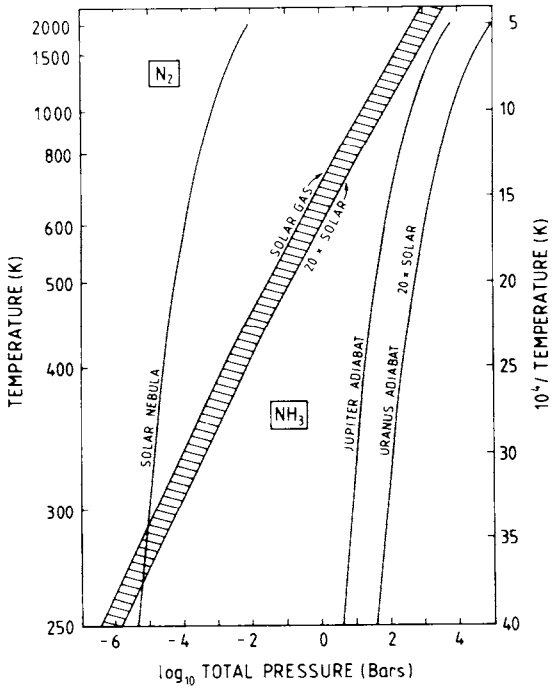

Fig. 10. The chemical equilibrium distribution of nitrogen between NH_3 and N_2 in solar composition gas as a function of temperature and pressure. The solar nebula, Jovian atmosphere and Uranian atmosphere (*P,T*) profiles are reproduced from Fig. 7. The shaded boundary is analogous to the $CH_4 - CO$ boundary in Fig. 7. Nonideality shifts the $NH_3 - N_2$ boundary to the left, thus decreasing the N_2/NH_3 ratio at a given temperature in the atmosphere of Uranus (figure modified from Fegley 1988*b*).

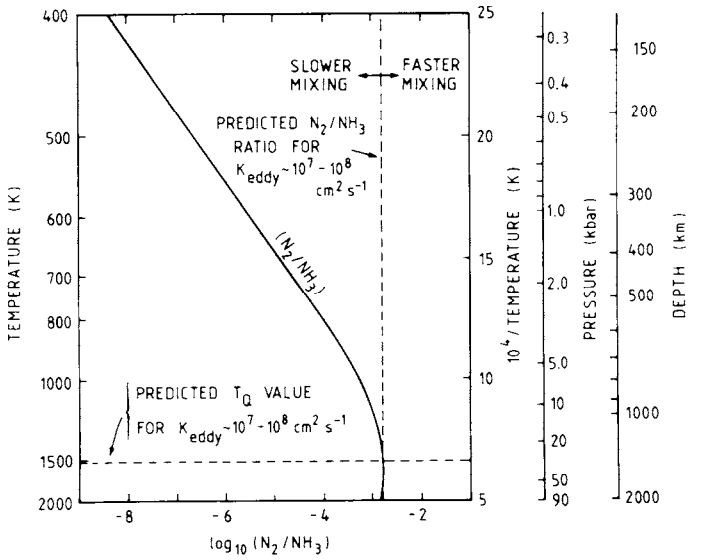

Fig. 11. An ideal gas chemical equilibrium calculation of the N_2/NH_3 ratio in the atmosphere of Uranus. The Uranus model adiabat and the vertical scales are the same as in Fig. 8. The range of N_2/NH_3 ratios and quench temperatures predicted for $K_{eddy} = 10^7$ to 10^8 $cm^2\ s^{-1}$ are so similar that they are shown as single lines. Nonideality will shift the calculated curve to the left thus giving smaller N_2/NH_3 ratios at each temperature (figure after Fegley 1990*a*).

noted that N_2 is potentially the most abundant nonequilibrium gas in the troposphere of Uranus. Furthermore, N_2 is potentially detectable by a suitably designed mass spectrometer on an entry probe mission. Therefore, it is important to understand the effects of the assumed vertical mixing rate and nitrogen elemental abundance on the N_2 abundance.

Figure 12, which is for the 20 times solar Uranus model, illustrates that the predicted N_2 mixing ratio is fairly insensitive to the assumed rate of vertical mixing in the deep atmosphere of Uranus and varies by less than a factor of 2 over the entire range of K_{eddy} values considered. Although, as noted earlier, the rate of vertical mixing on Uranus is uncertain, the replenishment of CH_4 destroyed by photochemistry requires some vertical mixing between the observable regions and the hot lower atmosphere where CH_4 is reformed (by equilibria such as Reactions 8 to 10) and N_2 is also produced. Thus, despite the apparent lack of an internal heat source on Uranus, a deep mixing source for tropospheric N_2 on Uranus appears inescapable.

However, the exact N_2 mixing ratio also depends upon the nitrogen elemental abundance. As discussed later in Sec.IV.F, the observed NH_3 depletion in the atmosphere of Uranus is more plausibly explained by a chemical mechanism than by the failure of Uranus to have accreted nitrogen-bearing materials. Thus we can examine the effects of variable nitrogen elemental enrich-

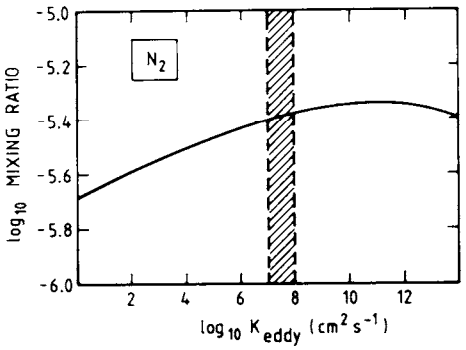

Fig. 12. Predicted N_2 mixing ratios as a function of the vertical eddy diffusion coefficient K_{eddy}. The shaded region at $K_{eddy} = 10^7$ to 10^8 cm^2 s^{-1} is appropriate for assumed convective heat fluxes of 10 to 100 erg cm^{-2} s^{-1}. Consideration of nonideality effects will reduce the N_2 mixing ratios by about a factor of 5. Note that the N_2 mixing ratio is relatively insensitive to K_{eddy} and varies by only a factor of 2 for the entire range of K_{eddy} values shown (figure after Fegley 1990*a*).

ments on the N_2 mixing ratio produced by vertical mixing. These results are displayed in Fig. 13. Because the NH_3 to N_2 conversion is quenched at temperatures of about 1500 K, the expected solubility of NH_3 in the aqueous solution clouds, which form at lower temperatures, does not affect these results.

The important point illustrated by Figs. 12 and 13 is that, in principle, N_2 is a sensitive indicator of the total nitrogen abundance in the atmosphere of Uranus. The N_2 mixing ratio is insensitive to the (uncertain) vertical mixing rate, but $X_{N_2} \propto X^2_{NH_3}$ (as shown by Eq. 15). Also, the observed NH_3 depletion in the 150 to 200 K region, well below the penetration depth of solar ultraviolet photons capable of photodissociating NH_3, rules out N_2 production by photochemistry. Furthermore, possible confusion with mass 28 peaks from CO or from C_2H_4 in a mass spectrometer is unlikely owing to the low predicted CO and C_2H_4 abundances. Finally, observations of NH_3 by a mass spectrometer on an entry probe probably will not be representative of the nitrogen abundance in the lower atmosphere below the predicted NH_4SH and aqueous solution clouds (unless the probe penetrates to these great depths). Therefore, a N_2 abundance determination may give us the "best" number for the nitrogen elemental abundance in the atmosphere of Uranus.

C. Other Chemical Probes

Ideal gas thermodynamic equilibrium calculations supplemented where possible by chemical kinetic calculations suggest that several other gases, in addition to CO and N_2, are potential chemical probes of the deep atmosphere of Uranus. As noted by Fegley and Prinn (1985*b*,1986), these gases include HCN, PH_3, CO_2, GeH_4, C_2H_6, CH_3SH, CH_3NH_2, CH_3OH, H_2Se, HCl, and HF. Arsine (AsH_3), which is a chemical probe of the deep atmospheres of

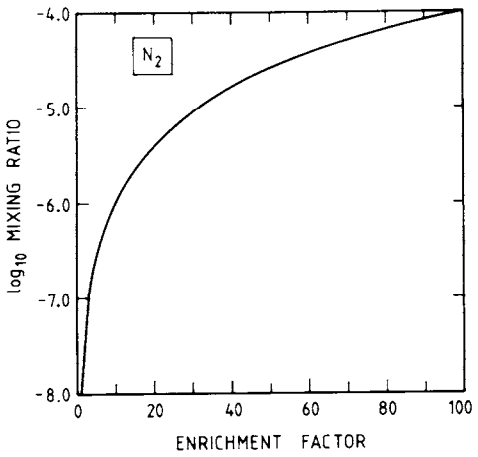

Fig. 13. Predicted N_2 mixing ratios as a function of the assumed nitrogen elemental enrichment over solar composition. A K_{eddy} value of 10^7 cm^2 s^{-1} was assumed. Consideration of nonideality effects will reduce the N_2 mixing ratios by about a factor of 5. At a constant quench temperature and pressure $X_{N_2} \propto X_{NH_3}^2$ and thus X_{N_2} varies with the square of the nitrogen elemental enrichment factor. Similar calculations presented in Fegley and Prinn (1986, Table VI) are for a different compositional model and for different (P,T) profiles (figure after Fegley 1990*a*).

Saturn and Jupiter (Fegley 1988*a*), is also a potential chemical probe of the deep atmosphere of Uranus.

Figures 9 and 14 show the ideal gas thermodynamic equilibrium abundances of these potential chemical probes for the 20 times solar Uranus model. Quench temperatures (T_Q) and mixing ratios at T_Q, calculated as described previously by Fegley and Prinn (1985*a*,*b*,1986), are shown for several gases and are also listed in Table III. Several important points are illustrated by these results. First, C_2H_6 is potentially the second most abundant disequilibrium species (after N_2) in the troposphere of Uranus. If C_2H_6 is quenched at 1000 K, the quench temperature estimated for ethane on Jupiter by Lewis and Fegley (1984), its mixing ratio is $\sim 4 \times 10^{-8}$. Similarly, if quenching of CH_3SH, CH_3NH_2 and CH_3OH also occurs at 1000 K, significant abundances of these gases will also result. However, the abundances of these four species, as well as the abundances of HCN, CO_2, GeH_4, AsH_3 and PH_3, are severely limited by condensation in the cold Uranian upper atmosphere. For reference, Fegley and Prinn (1986) used vapor pressure data from Stull (1947) to calculate that mixing ratios at the 74 K level (1 bar in their model) are $\sim 10^{-20}$ (HCN), $\sim 10^{-15}$ (CH_3SH), $\sim 10^{-12}$ (CO_2), $\sim 10^{-7}$ (PH_3) and $\leq 10^{-6}$ (GeH_4). Thus a mass spectrometer on an entry probe capable of penetrating deeper into the warmer troposphere appears to be the best method for detecting many of the gases listed in Table III.

Second, some potential chemical probes such as C_2H_6, CH_3SH, CH_3NH_2, CH_3OH, HCN and CO_2 display steep temperature dependences and

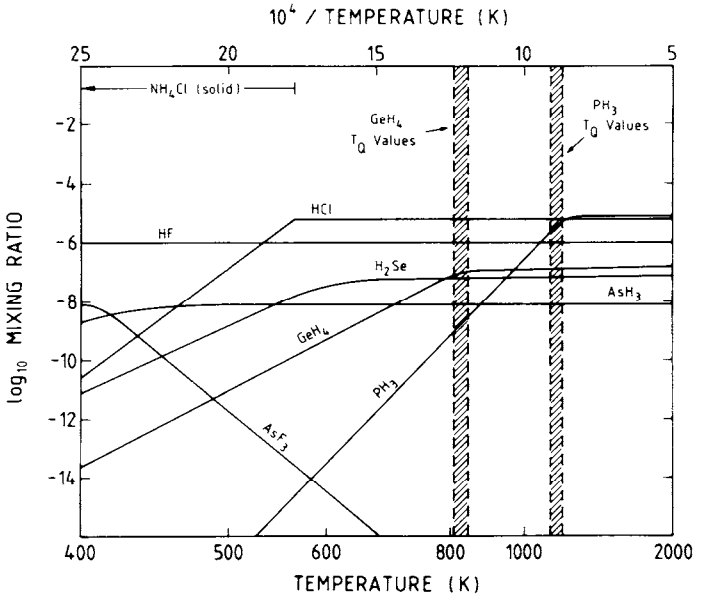

Fig. 14. As in Fig. 9 but for important Cl, F, Ge, Se and As-bearing gases. NH_4Cl (solid) condenses at 560 K and NH_4F (solid) condenses at 396 K. Both compounds presumably will dissolve in the aqueous solution cloud which forms at 463 K. The vertical shaded regions show calculated PH_3 and GeH_4 quench temperatures (T_Q) appropriate for K_{eddy} values of 10^7 to 10^8 cm^2 s^{-1}. The corresponding mixing ratios at T_Q for these gases are also given in Table III. Again, observations of several of these species may be possible with a suitably designed mass spectrometer on an entry probe (figure after Fegley 1990*b*).

are thus also sensitive to the vertical mixing rate in the deep atmosphere of Uranus. This sensitivity has been studied quantitatively for HCN and CO_2 by Fegley and Prinn (1985*b*, 1986). In principle, similar quantitative calculations are also possible for C_2H_6, CH_3SH, CH_3NH_2 and CH_3OH. However, other chemical probes such as HCl, HF, H_2Se and AsH_3 are fairly insensitive to temperature (and thus to the vertical mixing rate) over fairly wide ranges. Observations of these species are desirable because they are predicted to be the major gases containing Cl (HCl), F (HF), Se (H_2Se) and As (AsH_3).

Both PH_3 and GeH_4 are intermediate cases; quenching at high temperatures (caused by rapid vertical mixing) will occur where their abundances are essentially temperature independent. In this region, PH_3 is also the dominant phosphorus-bearing gas and the PH_3/H_2 mixing ratio is equivalent to the total P/H_2 mixing ratio. However, quenching at lower temperatures (caused by slower vertical mixing) will occur where the PH_3 and GeH_4 abundances are steep functions of the temperature. In fact, this case is more likely to occur. As Fig. 14 illustrates K_{eddy} values of 10^7 to 10^8 cm^2 s^{-1} lead to quenching of PH_3 and GeH_4 at the points where the abundances of these two gases start to

TABLE III
Predicted Mixing Ratios of Chemical Probes on Uranus[a]

Probe	Quench Temperature (K)	Mixing Ratio
N_2	1456–1513[b]	$(4.1\text{-}4.3) \times 10^{-6}$
HCN	1318–1372	$(6.3\text{-}13) \times 10^{-11}$
PH_3	1098–1145	$(1.9\text{-}4.5) \times 10^{-6}$
CO	854–895[b]	$(1.0\text{-}3.2) \times 10^{-11}$
CO_2	830–875	$(5.0\text{-}13) \times 10^{-13}$
GeH_4	807–842	1.1×10^{-7}
AsH_3	1222–1286	8.2×10^{-9}
C_2H_6	1000[c]	3.7×10^{-8}
CH_3SH	1000[c]	1.3×10^{-9}
CH_3NH_2	1000[c]	2.6×10^{-10}
CH_3OH	1000[c]	1.7×10^{-10}

[a]Predictions assume 20 times solar composition and $K_{eddy} = 10^7 - 10^8$ cm^2 s^{-1}. These are ideal gas thermochemical equilibrium calculations. As discussed by Fegley and Prinn (1986), nonideality effects will decrease the N_2, CO, CO_2 and HCN abundances and will increase the PH_3 and GeH_4 abundances (Table after Fegley 1990*b*).

[b]Homogeneous gas phase reactions only are considered because the presence of Fe particles in the deep atmosphere is very unlikely as shown by Fegley and Prinn (1986). Heterogeneous reactions were considered by Fegley and Prinn (1985*b*).

[c]A quench temperature of 1000 K is assumed for these species for illustrative purposes.

decrease steeply with decreasing temperature. Slower vertical mixing will thus yield smaller PH_3 and GeH_4 abundances.

D. Deuterated Gases

As mentioned previously in Sec.III.B.5, CH_3D has been observed on Uranus and several attempts have also been made to observe HD. The abundances of HD, CH_3D and of other potentially observable monodeuterated species (e.g., HDO, NH_2D, HDS) are related via the net thermochemical reactions

$$CH_4 + HD = CH_3D + H_2 \quad (16)$$

$$H_2O + HD = HDO + H_2 \quad (17)$$

$$NH_3 + HD = NH_2D + H_2 \quad (18)$$

$$H_2S + HD = HDS + H_2 \quad (19)$$

which have equilibrium constants given by the expressions

$$K_{16} = [(X_{CH_3D}X_{H_2})/(X_{CH_4}X_{HD})][(\phi_{CH_3D}\phi_{H_2})/(\phi_{CH_4}\phi_{HD})] \quad (20)$$

$$K_{17} = [(X_{HDO}X_{H_2})/(X_{H_2O}X_{HD})][(\phi_{HDO}\phi_{H_2})/(\phi_{H_2O}\phi_{HD})] \quad (21)$$

$$K_{18} = [(X_{NH_2D}X_{H_2})/(X_{NH_3}X_{HD})][(\phi_{NH_2D}\phi_{H_2})/(\phi_{NH_3}\phi_{HD})] \quad (22)$$

$$K_{19} = [(X_{HDS}X_{H_2})/(X_{H_2S}X_{HD})][(\phi_{HDS}\phi_{H_2})/(\phi_{H_2S}\phi_{HD})]. \quad (23)$$

To a very good first approximation the fugacity coefficients of isotopically substituted gases are identical (e.g., $\phi_{HD} = \phi_{H_2}$, $\phi_{CH_3D} = \phi_{CH_4}$, etc.) and the equilibrium constant expressions (20) to (23) therefore reduce to the mixing ratio quotients.

The equilibrium constants for Reactions (16) to (19) can be calculated from thermodynamic data tabulated in the JANAF Tables or in other compilations (see, e.g., Richet et al. 1977). Then by assuming a bulk D/H atom ratio for the Uranus atmosphere it is possible to calculate the abundances of deuterated species such as CH_3D, HDO, NH_2D, HDS, etc. This has already been done for Jupiter and Saturn by Fegley and Prinn (1988*b*), who described the computational methods in detail.

It is convenient to express the results of these calculations in terms of the deuterium fractionation factor α which is defined as

$$\alpha_{gas} = [(D/H)_{gas}]/[(D/H)_{H_2}] \quad (24)$$

where the terms in parenthesis denote the D to H atom ratios in the two gases and the subscript stands for CH_4, H_2O, NH_3, etc. The fractionation factor α and the equilibrium constant K for deuterium exchange equilibria such as Reactions (16) to (19) are related to each other by expressions such as

$$K_{16} = 2\alpha_{16} \quad (25)$$

$$K_{17} = \alpha_{17} \quad (26)$$

$$K_{18} = 1.5\alpha_{18} \quad (27)$$

$$K_{19} = \alpha_{19} \quad (28)$$

where the proportionality constants depend on the ratio of exchangeable H atoms in H_2 and the respective hydride. Both the equilibrium constants and the fractionation factors for deuterium exchange equilibria are temperature dependent.

The relationships between the α values and the equilibrium constants combined with the fact that the bulk D/H value = $1/2(HD/H_2)$ allow us to transform Eqs. (20) to (23) into the following equivalent expressions for the bulk (D/H) value on Uranus

$$(D/H) = (X_{CH_3D}/X_{CH_4})/4\alpha_{16} \quad (29)$$

$$(D/H) = (X_{HDO}/X_{H_2O})/2\alpha_{17} \quad (30)$$

$$(D/H) = (X_{NH_2D}/X_{NH_3})/3\alpha_{18} \quad (31)$$

$$(D/H) = (X_{HDS}/X_{H_2S})/2\alpha_{19}. \quad (32)$$

Determination of monodeuteride to hydride ratios [e.g., (CH_3D/CH_4)] in the atmosphere of Uranus thereby yield the bulk (D/H) ratio provided that the value of the appropriate fractionation factor [e.g., α_{16} for (CH_3D/CH_4)] is known.

Figures 15 to 17 and Table IV present calculations of the methane, water vapor, and ammonia fractionation factors on Uranus (Fegley 1990*c*). The temperature dependence of the fractionation factors means that the α values

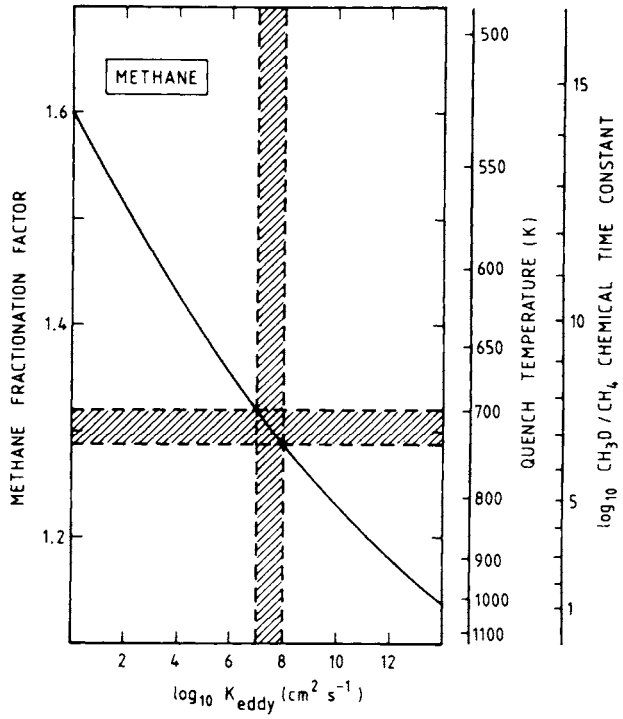

Fig. 15. Predicted fractionation factors for deuterium exchange between CH_4 + HD in the atmosphere of Uranus as a function of the vertical eddy diffusion coefficient K_{eddy}. The fractionation factor is defined as the D/H atom ratio in methane relative to the D/H atom ratio in hydrogen. The calculated quench temperatures and chemical time constants for CH_3D formation via homogeneous gas phase deuterium exchange are also shown. The shaded region at $K_{eddy} = 10^7$ to 10^8 cm^2 s^{-1} is appropriate for assumed convective heat fluxes of 10 to 100 erg cm^{-2} s^{-1} (Danielson 1977; Hubbard 1978). The predicted fractionation factors are independent of the assumed elemental enrichments over solar composition, the assumed D/H ratio, and nonideality effects (figure after Fegley 1990*c*).

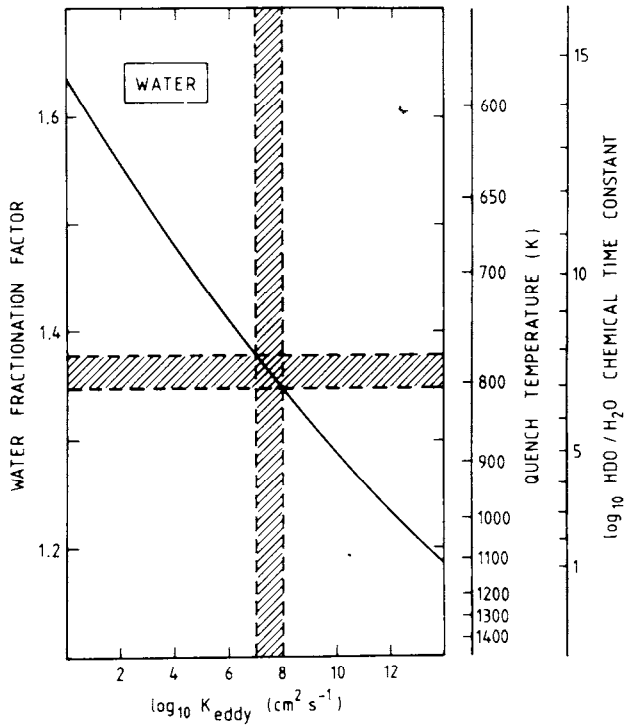

Fig. 16. As in Fig. 15 but for deuterium exchange between H_2O + HD (figure after Fegley 1990*c*).

for Reactions (16) to (19) also depend on the assumed vertical mixing rate, with more rapid vertical mixing causing quenching at higher temperatures where the α values are smaller and less rapid vertical mixing causing quenching at lower temperatures where the α values are larger.

As noted by Fegley (1990*c*), the calculated quench temperatures and deuterium fractionation factors are independent of the assumed (D/H) ratio and the assumed elemental enrichments over solar composition. Taking the methane fractionation factor (α_{16} = 1.32) appropriate for K_{eddy} = 10^7 cm^2 s^{-1} from Table IV, we can use the (CH_3D/CH_4) ratio of $\sim 3.6 \times 10^{-4}$ reported by de Bergh et al. (1986) to estimate the Uranus D/H value. The resulting value of (D/H) $\sim 7 \times 10^{-5}$ is slightly lower than (but within the uncertainties of) the value derived by de Bergh et al. (1986). However, (D/H) $\sim 7 \times 10^{-5}$ is best regarded as a provisional value because of the uncertainties associated with the strength of vertical mixing in the deep atmosphere of Uranus. In particular, as illustrated in Fig. 15, the larger α values resulting from weaker vertical mixing will lead to smaller calculated (D/H) values. Thus, as suggested in Sec. V, it is important to determine both the (HD/H_2) and the (CH_3D/CH_4) ratios with sufficient accuracy and precision to derive

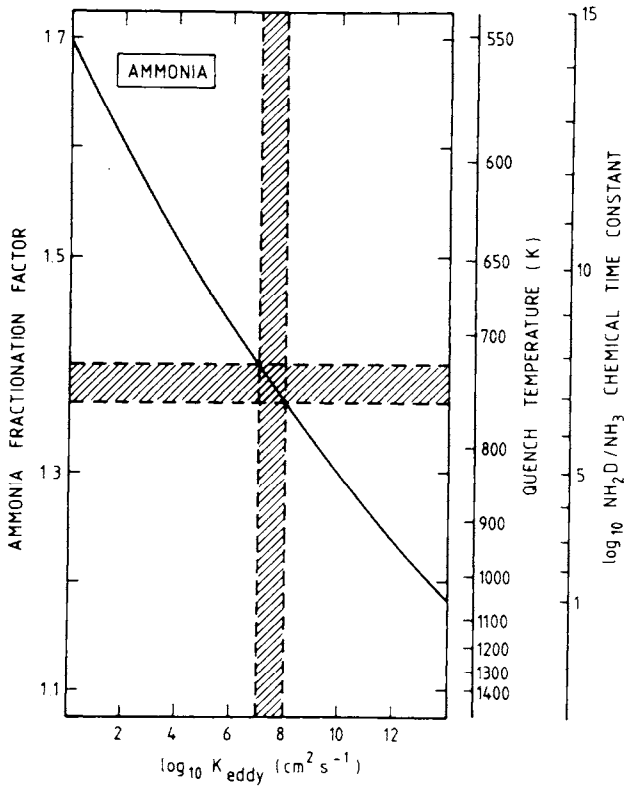

Fig. 17. As in Fig. 15 but for deuterium exchange between NH_3 + HD (figure after Fegley 1990*c*).

the methane fractionation factor empirically. Once this is done, the calculated α value can be used in conjunction with the results presented in Fig. 15 to constrain the K_{eddy} value in the deep atmosphere of Uranus.

E. Water Cloud Condensation

Oxygen is the third most abundant element after hydrogen and helium and H_2O is therefore expected to be the third most abundant gas after H_2 and He in the deep atmospheres of Jupiter, Saturn, Uranus and Neptune. Water cloud condensation in the deep atmosphere of Uranus has been discussed by a number of authors (see, e.g., Atreya and Romani 1985; Carlson et al. 1987*a*,1988; de Pater et al. 1989; Fegley 1990*d*; Fegley and Prinn 1985*b*,1986; Lewis 1974*a*; Romani 1986; Stevenson 1984*b*; Weidenschilling and Lewis 1973) because of its important chemical, dynamical and physical implications.

Water cloud condensation on Uranus is predicted to occur at higher temperatures (and therefore at deeper levels) than in the atmospheres of Jupiter

TABLE IV
Predicted Fractionation Factors for (D/H) Exchange on Uranus[a]

Gas	Quench Temperature	Fractionation Factor[b]	Predicted Mixing Ratio[c]
CH_3D	699–732	1.321–1.290	$(7.2\text{-}7.1) \times 10^{-6}$
HDO	773–808	1.376–1.345	$(6.6\text{-}6.3) \times 10^{-6}$
NH_2D	724–758	1.399–1.362	1.2×10^{-6}

[a]Predictions are for homogeneous gas phase reactions. A 20 times solar model with $K_{eddy} = 10^7 - 10^8$ cm^2 s^{-1} is used (Table after Fegley 1990*c*).
[b]The predicted fractionation factors are independent of the assumed elemental enrichment factor, the assumed (D/H) ratio, and nonideality effects.
[c]The predictions assume (D/H) = 10^{-4} for Uranus. The abundances of the monodeuterides scale linearly with the D/H atom ratio.

and Saturn because of the larger amounts of water vapor expected in the deep atmosphere of Uranus. Figure 18 illustrates predicted temperatures for water cloud condensation as a function of the water enrichment factor over solar composition. These calculations, taken from Fegley (1990*d*), were performed assuming equal enrichments for all elements except H, He and Ne and taking $P = 1$ bar at 76 K (Lindal et al. 1987). The position of the water cloud base was then calculated using the expression for the wet adiabatic lapse rate from Lasker (1963) and vapor pressure data for CH_4 (Angus et al.

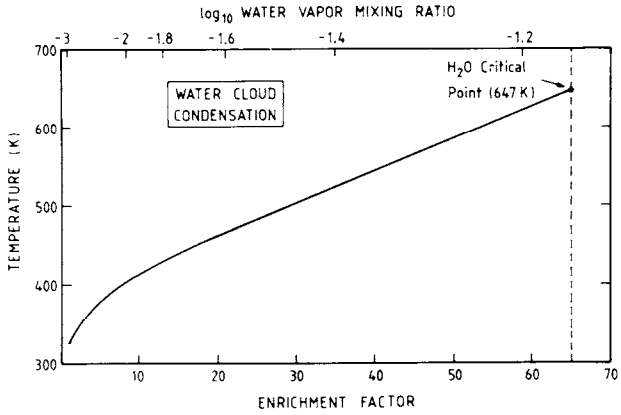

Fig. 18. Water cloud condensation temperatures as a function of the assumed elemental enrichment over solar composition. An enrichment of 65 times solar leads to water cloud condensation at the critical temperature of 647 K. Larger enrichments of the water abundance cannot produce condensation at higher temperatures and lead instead to condensation of larger amounts of water at 647 K. Fegley and Prinn (1986) have about the same water vapor mixing ratio at the critical point but give an enrichment factor of 120 times. They assumed that about 32% of all oxygen was in rocky material instead of being in H_2O. Thus, $120 \times 0.68 \times (1.38 \times 10^{-3}) \sim 0.11$ vs $65 \times (1.38 \times 10^{-3}) \sim 0.09$ for the H_2O mixing ratio required for critical point condensation (figure after Fegley 1990*d*).

1976; Kelley 1935), water ice (Mason 1971*b*) and liquid water (Keenan et al. 1969). These calculations, which account for the effect of both CH_4 and H_2O clouds on the adiabatic lapse rate, are compared with those by other authors in Table V; Fig. 19 illustrates the variation of the H_2O mixing ratio above the water cloud base for the 20 times solar Uranus model atmosphere.

Figure 18 and Table V show that a sufficiently large enrichment of the H_2O/H_2 mixing ratio over solar composition (1.38×10^{-3}) leads to water cloud condensation at the critical point (647 K). This behavior was first noted by Fegley and Prinn (1985*b*) and was later re-emphasized by Fegley and Prinn (1986) who calculated that the H_2O/H_2 mixing ratio required for water cloud condensation at the critical point is $\sim$ 11%. The more recent calculations by Fegley (1990*d*), reproduced in Fig. 18 and Table V, yield H_2O/H_2 $\sim$ 9% in good agreement with the previous results. This mixing ratio corresponds to 65 times the solar H_2O/H_2 ratio. (We note that Fegley and Prinn gave the corresponding enrichment factor as 120 times solar. However, their model assumed that 32% of the solar oxygen abundance was incorporated in hydrated rocky material inside Uranus. Thus, $120 \times 0.68 \times (1.38 \times 10^{-3}) \sim 0.11$ vs $65 \times (1.38 \times 10^{-3}) \sim 0.09$ for the two calculated H_2O/H_2 mixing ratios at the critical point.)

However, as pointed out by Fegley and Prinn (1986), continued increases in the H_2O/H_2 mixing ratio (above the critical value of $\sim$ 9%) do not lead to water cloud condensation at higher temperatures. Instead, large sudden decreases in the H_2O/H_2 mixing ratio occur associated with the onset of water cloud condensation at 647 K (e.g., see, Fegley and Prinn [1986, Fig. 8] for an example of this behavior).

TABLE V
Water Cloud Condensation on Uranus

Enrichment Factor	Cloud Base Temperature (K)		
	Fegley (1990*d*)[a]	Romani (1986)	Carlson et al. (1987*a*)
1	325	318	320
10[b]	414	407	386
20	463	456	416
30	504	503	—
50	584	—	—
65[c]	647	—	—

[a] Water vapor pressure data are taken from Keenan et al. (1969).

[b] Weidenschilling and Lewis (1973) give the aqueous solution cloud base temperature as ~390 K.

[c] (H_2O/H_2) ~9% leads to condensation at the critical point of water (647 K). Fegley and Prinn (1986) have about the same water vapor mixing ratio (~10.5%) at the critical point but give an enrichment factor of 120 times. They assumed that about 32% of all oxygen was in hydrated rocky material instead of water vapor. Thus, $120 \times 0.68 \times (1.38 \times 10^{-3}) \sim 0.11$ vs $65 \times (1.38 \times 10^{-3}) \sim 0.09$ in the present model. Different (P, T) profiles account for the factor of ~1.2 difference between the results.

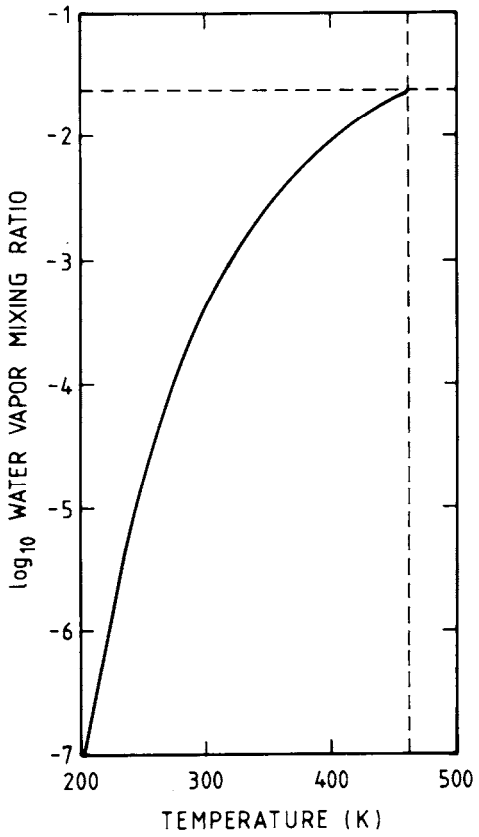

Fig. 19. Water vapor mixing ratio as a function of temperature for the 20 times solar Uranus model (figure after Fegley 1990*d*).

Below the water cloud base at 647 K, a supercritical water fluid will exist. Supercritical water is a highly corrosive solvent which dissolves many inorganic compounds including rock-forming minerals. As Lewis (1974*a*) has pointed out, mineral solubilities in supercritical water increase with increasing temperature and also with increasing pressure. The latter behavior results from the exponential increase of the thermodynamic activity of minerals with increasing pressure:

$$\ln a_i = \int_{P_1}^{P_2} \left(\frac{V_i}{RT}\right) dP \tag{33}$$

where a_i is the thermodynamic activity of mineral i, V_i is the molar volume of mineral i, R is the gas constant, P_1 is 1-bar pressure, and P_2 is the pressure at some level in the deep atmosphere of Uranus. Thus, pressures of about 10^4

to 10^5 bar yield thermodynamic activities of $\sim 10^4$ to 10^6 (instead of the conventional 1-bar value of unity). These greatly enhanced activities mean that the minerals are $\sim 10^4$ to 10^6 times more soluble than they are at 1 bar pressure (e.g., see Lewis 1974*a*, Fig. 2-20). For example, silica solubility in water increases from $\sim$ 6.0 ppm at room temperature and pressure (Morey et al. 1962) to $\sim$ 750 g per kilogram of fluid at $\sim$ 1353 K and 9.7 kbar where SiO_2-fluid-melt are in equilibrium (Kennedy et al. 1962). More complex minerals such as enstatite ($MgSiO_3$), albite ($NaAlSi_3O_8$) and diopside ($CaMgSi_2O_6$), which are constituents found in chondritic material, also readily dissolve in supercritical water (e.g., see Morey 1957; Holland and Malinin 1979).

Another consequence of water cloud condensation at the critical point may be the formation of an "ionic ocean" in the deep atmosphere of Uranus. Lewis (1974*a*) also suggested that the presence of NH_3 on Uranus may lead to reactions exemplified by

$$2H_2O\ (\text{fluid}) + 4NH_3 + SiO_2 = 4NH_4^+\ (\text{fluid}) + SiO_4^{4-}\ (\text{fluid}) \quad (34)$$

which may further enhance the solubility of "rocky" materials in supercritical water. Stevenson and Fishbein (1981) independently suggested that water self-dissociation

$$2H_2O\ (\text{fluid}) = H_3O^+\ (\text{fluid}) + OH^-\ (\text{fluid}) \quad (35)$$

at high temperatures and pressures may lead to an "ionic ocean" in the deep atmosphere of Uranus. Subsequent reactions exemplified by

$$2H_3O^+\ (\text{fluid}) + FeO = Fe^{2+}\ (\text{fluid}) + 3H_2O\ (\text{fluid}) \quad (36)$$

$$2H_3O^+\ (\text{fluid}) + MgO = Mg^{2+}\ (\text{fluid}) + 3H_2O\ (\text{fluid}) \quad (37)$$

$$4OH^-\ (\text{fluid}) + SiO_2 = SiO_4^{4-}\ (\text{fluid}) + 2H_2O\ (\text{fluid}) \quad (38)$$

may also lead to increased dissolution of "rocky" phases. These qualitative considerations and measured mineral solubilities in supercritical water have led several authors to suggest that the "rocky" component inside Uranus is soluble (to some extent) in the "atmosphere" (Lewis 1974*a;* Stevenson 1985; Fegley and Prinn 1986).

Several interesting dynamical and physical consequences may also result from critical point condensation. It is well known that the heat of vaporization for the liquid $\rightarrow$ vapor phase change goes to zero at the critical point as the distinction between the two phases vanishes (Keenan et al. 1969; Levelt Sengers 1977). In this case the wet and dry lapse rates will be identical. This can easily be illustrated by considering the equation for the wet lapse rate given by Lewis (1969)

$$(\partial T/\partial Z)_S = -\bar{\mu}g/[C_p + (\Delta H_{vap})X_w(\Delta H_{vap}/RT^2 - 1/T)] \quad (39)$$

where $\bar{\mu}$ is the mean molecular weight of atmospheric gas and X_w is the water vapor mixing ratio. As the heat of vaporization $\Delta H_{vap} \rightarrow 0$, then $(\partial T/\partial Z)_S \rightarrow -\bar{\mu}g/C_p$, the dry lapse rate. We also note that, unlike other clouds on the Earth and on the giant planets, no precipitation is possible from any water cloud forming at the critical point because there is no physical distinction between the "raindrop" and the supercritical water fluid below the cloud base.

Other thermodynamic properties such as the isothermal compressibility β_T, the heat capacities at constant pressure C_p and constant volume C_v, the isobaric thermal expansion coefficient α_p, and the sound speed show anomalies at the critical point. The same is true for transport properties (e.g., viscosity and thermal conductivity) and for the Rayleigh and Prandtl numbers. Levelt Sengers (1977) has noted that the large increases (in some cases 9 orders of magnitude over the dilute gas) in the Rayleigh number may greatly increase the tendency toward convection.

Fegley and Prinn (1986) briefly discussed possible dynamical consequences of water cloud condensation at the critical point. They noted that the condensation of a significant fraction of the available water, which will occur for H_2O/H_2 mixing ratios significantly above the critical value of 9%, will lead to a sudden decrease in the mean molecular weight of atmospheric gas. Assuming that the condensate is not entrained in the upwardly moving gas parcel, the decrease in $\bar{\mu}$ and in the mean atmospheric density $\bar{\rho}$ will result in a large upward buoyancy force (F_b) and acceleration ($\partial^2 Z/\partial t^2$) given by

$$F_b \sim g(\bar{\rho}_{amb} - \bar{\rho}_{mov}) \quad (40)$$

$$\partial^2 Z/\partial t^2 \sim g[(\bar{\mu}_{amb}/\bar{\mu}_{mov}) - 1] \quad (41)$$

where the subscripts refer to ambient and moving gas parcels (i.e., before and after water vapor condensation). For their 500 times solar model Uranus atmosphere, Fegley and Prinn (1986) calculated $\Delta\bar{\rho} \sim 0.2$ g cm^{-3} and $(\bar{\mu}_{amb}/\bar{\mu}_{mov}) \sim 1.8$, corresponding to an upward buoyancy acceleration of ~ 0.8 g. They further noted that both the increased Rayleigh number and the decreased mean molecular weight qualitatively indicated enhanced vertical transport at the critical point water cloud base.

Gierasch and Conrath (1987) also point out that a variation in the concentration of a condensible species (such as CH_4 or H_2O) with a molecular weight greater than that of "dry" atmospheric gas can have a strong effect on convection. However, they argue that the molecular weight variations caused by condensation will lead to the formation of "thin" layers (relative to the scale height) of uniform composition and with diffusively controlled stable interfaces. This structure is predicted by them to decrease vertical transport. The apparent discrepancy between their predictions (which do not explicitly

consider critical point condensation) and those of Fegley and Prinn (1986) clearly warrant further study beyond the scope of this review. However, as noted previously, we emphasize that some vertical mixing is required to replenish the CH_4 destroyed by solar ultraviolet photolysis in the upper Uranian atmosphere. Furthermore, as Fig. 12 illustrates, even very slow vertical mixing is predicted to provide significant amounts of N_2 in the troposphere of Uranus.

F. Ammonia Depletion Mechanisms

Another potentially important consequence of water cloud condensation is its effect on the abundances of soluble gases. The case of ammonia will be discussed first, and then the effects on other gases (including several species such as H_2 and CH_4 that are generally regarded as being insoluble in water) will be described in the next section.

The dissolution of NH_3 in water is given by the reaction

$$NH_3(g) = NH_3(aq) \tag{42}$$

which has the equilibrium constant

$$K_{42} = H_{NH_3} = [NH_3(aq)]/P_{NH_3} \tag{43}$$

where H_{NH_3} is the Henry's Law constant for NH_3 and has units of molal bar^{-1}, (aq) denotes an aqueous solution, and $[i(aq)]$ denotes the concentration of species i in an aqueous solution in terms of molality (moles of solute per kg of solvent). The molal concentration can be transformed to the corresponding mole fraction by dividing by 55.51, the number of moles of liquid water in 1 kg of aqueous solution. Thus, rearranging Eq. (43) to solve for the mole fraction of aqueous ammonia $X_{NH_3}(aq)$ yields

$$X_{NH_3}(aq) = (H_{NH_3} \cdot P_{NH_3})/55.51 \tag{44}$$

for Eq. (42) above.

The Henry's Law constant is temperature dependent; however, unlike many chemical equilibrium constants, it cannot be extrapolated to higher temperatures using the second law of thermodynamics ($\log_{10}H$ vs $1/T$). This treatment, which has been done by other authors (see, e.g., Carlson et al. 1987*a*), is incorrect because gas solubilities generally decrease, go through a minimum, and then increase as temperature increases toward the solvent's critical temperature (e.g., see Clever and Han 1980; Mason and Kao 1980; Hayduk and Laudie 1973; Schotte 1985; Shock et al. 1989). This behavior is schematically illustrated in Fig. 20.

Fegley (1990*e*) used the temperature dependent equation for H_{NH_3} given

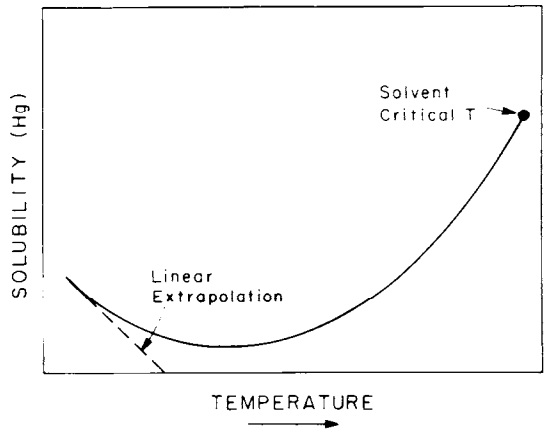

Fig. 20. A schematic diagram showing the effect of temperature on gas solubility in water. The solubility H_g is the equilibrium constant for the general reaction G(gas) = G(aqueous). Gas solubilities generally decrease to a minimum value and then increase again as the temperature is increased up to the critical point (647 K) (e.g., see Shock et al. 1989). This behavior has important consequences for calculated gas solubilities in aqueous solution clouds on Uranus. In particular, calculations based on linear extrapolations of room temperature solubility data generally underestimate the high temperature solubilities. See the text for a full discussion.

by Roberts and Tremaine (1985) to estimate the ammonia solubility in water clouds on Uranus. His results, reproduced in Table VI, show that the ammonia solubility reaches 9% (molar) in water clouds forming at the critical temperature (647 K). The same solubility at 647 K was also found by Fegley and Prinn (1986). However, substantially lower solubilities are calculated using the thermodynamic data from Carlson et al. (1987*a*) and from Romani (1986).

Table VI lists the Henry's Law constants calculated from the data given by these authors and the corresponding ammonia solubility values (for the same atmospheric models as used by Fegley 1990*e*). The Henry's Law constants calculated from the 298 K data in Carlson et al. (1987*a*) are smaller than those of Roberts and Tremaine (1985) because the Carlson et al. data are extrapolated to higher temperatures by the second law method ($\log_{10} H_{NH_3}$ vs $1/T$)—as done by Carlson et al. (1987*a*). As noted above, this linear extrapolation is incorrect. However, it is not obvious why the Henry's Law constants calculated from the data of Romani (1986) are also too small. One possible reason is that experimental errors in the measurements made by Wilson (1925)—which Romani (1986) used—increased with increasing temperature and led to underestimates of the Henry's Law constant. Rizvi (1985) recently reviewed Wilson's (1925) data and discussed several possible experimental errors. Another possibility is that Romani's extrapolation (via a 3 coefficient polynomial) of Wilson's data to temperatures above his highest experimental value (~ 360 K) leads to unreliable H_{NH_3} values. However,

TABLE VI
Ammonia Solubility Data and Ammonia Solubility in Water Clouds on Uranus

Water Enrichment Factor	Cloud Base Temperature	$\log_{10}$ Henry's Law Constant (Molal Bar^{-1})			Mole Fraction of Dissolved NH_3[d]		
		Fegley (1990*e*)[a]	Carlson et al. (1987*a*)[b]	Romani (1986)[c]	Fegley (1990*e*)	Carlson et al. (1987*a*)	Romani (1986)
1	325	+1.250	+1.249	+1.174	0.006	0.006	0.005
10	414	+0.147	+0.053	+0.095	0.012	0.009	0.010
20	463	−0.215	−0.409	−0.305	0.017	0.011	0.014
30	504	−0.428	−0.727	−0.572	0.024	0.012	0.017
50	584	−0.673	−1.218	−0.969	0.038	0.011	0.019
65	647	−0.749	−1.520	−1.201	0.092	0.017	0.035

[a]Fegley (1990*d*) took the $\log_{10}H = f(T)$ equation from Roberts and Treiman (1985).
[b]Carlson et al. (1987*a*) linearly extrapolated thermodynamic data at 298.15 K (see their Table 1) to higher temperature using the second law method.
[c]Romani (1986) lists coefficients for the NH_3 vapor pressure over aqueous ammonia solutions as a function of concentration. These yield the Henry's Law constant. However, note that he has given an incorrect vapor pressure equation (Appendix B of his thesis). The correct equation is $\ln P(NH_3) = A + B/T + C \ln T$.
[d]The mole fraction of dissolved NH_3 is calculated using the tabulated Henry's law constants and the NH_3 partial pressure corresponding to the different atmosphere models.

whatever the actual reason may be, it appears that at least some of the debate over the efficiency of NH_3 removal by aqueous solution clouds is due to the different (and incorrect) thermodynamic data used by the different authors. Although resolution of this disagreement is beyond the scope of this review, it is instructive to keep Table VI in mind while considering the different ammonia depletion mechanisms that have been proposed.

As mentioned earlier in Sec.IV.B, microwave observations indicate that the NH_3/H_2 mixing ratio in the 150 to 200 K region of the Uranian atmosphere is $\sim$ 100 to 200 times lower than the solar NH_3/H_2 mixing ratio of $\sim 1.74 \times 10^{-4}$ (de Pater and Gulkis 1988; de Pater and Massie 1985; de Pater et al. 1989; Gulkis et al. 1978,1983; Hofstadter and Muhleman 1989; Klein and Turegano 1978). This depletion could reflect a planetary depletion in nitrogen (e.g., as suggested by Lewis and Prinn [1980]), a chemical mechanism for removing NH_3 from the Uranian atmosphere, or a combination of both. In fact, all three models have been proposed in the literature.

Considering a planetary depletion of nitrogen first, Figs. 7 and 10 show that the accretion of Uranus involves the chemical reprocessing of CO and N_2 into CH_4 and NH_3. This is true regardless of the CO and N_2 being nebular or interstellar and of the reprocessing occurring in a circum-Uranian subnebula or in the absence of such a subnebula. The observed enrichment of CH_4, coupled with the greater volatility of CH_4 and of CH_4 clathrate (ideally $CH_4 \cdot 6H_2O$) relative to that of NH_3 and of NH_3 hydrate ($NH_3 \cdot H_2O$), argues that any nitrogen depletion during the accretion process must occur while

nitrogen is still present as N_2. However, since both CO and N_2 ices and clathrates have similar volatilities, such a depletion involves either a very good nebular thermostat or accretion of carbon as disequilibrium organic material such as that found in the carbonaceous chondrites. Given the difficulties in the kinetics of CO and N_2 clathrate formation in the solar nebula (Fegley 1988*b*), and the apparent problems in producing nebular temperatures low enough for condensation of CO and N_2 ices ($T \leq 20$ K), the second mechanism involving disequilibrium organic matter may be more likely. However, this mechanism alone is not sufficient to account for the inferred NH_3 depletion because the N/C atomic ratio in Type 1 carbonaceous chondrites is ~ 0.07 (Mason 1971*a*) while the upper limit on the NH_3/CH_4 ratio in the 150 to 200 K region of the Uranian atmosphere is $\sim 8 \times 10^{-5}$ or about 900 times smaller. Thus a chemical mechanism for NH_3 depletion in the Uranian atmosphere also appears necessary.

Atreya and Romani (1985) first proposed that NH_3 dissolution in aqueous solution clouds was the mechanism responsible for the inferred NH_3 depletion. Quoting Romani (1986): "Model predictions are compared to relevant observations. In particular, the observed NH_3 depletion on Uranus is consistent with loss into an extensive $NH_3 - H_2O$ solution cloud, and it is not necessary to selectively enrich H_2S to NH_3." However, this conclusion was subsequently challenged by Carlson et al. (1987*a*) who presented their own calculations showing that only 20 to 30% of the NH_3 was removed by the aqueous solution clouds, thus leaving too much NH_3 in the 150 to 200 K region of the Uranian atmosphere. In this regard, it is instructive to recall that the second-law extrapolation utilized by Carlson et al. underestimates the true NH_3 solubility. But as Table VI shows, their calculated NH_3 solubility for a 20 times solar model is only $\sim$ 30% lower than that of Romani (1986). This difference is too small to account for the different claims made by the two groups. Carlson et al. (1987*a*) also reiterated the earlier suggestion of Prinn and Lewis (1973) and Weidenschilling and Lewis (1973) that formation of NH_4SH clouds could account for the inferred NH_3 depletion, provided that the H_2S/NH_3 ratio in the atmosphere of Uranus was enhanced by a factor of 4 above the solar value of ~ 0.2. However, Carlson et al. (1987*a*) failed to present a plausible mechanism for accomplishing this enrichment.

The recent paper by de Pater et al. (1989) re-examines NH_3 loss by aqueous solution clouds and by NH_4SH formation and concludes that "The decrease in the ammonia mixing ratio is caused primarily by the formation of an NH_4SH cloud, although a fair fraction ($\sim$ 65%) will get lost in the solution cloud if water is enhanced by a factor of $>$ 500 above the solar value." These authors also reiterated the earlier suggestions that the S/N ratio must be enhanced above the solar value for NH_4SH formation to be effective in removing NH_3 from the upper atmosphere. Furthermore, de Pater et al. (1989) proposed that the observed latitudinal variation in the NH_3 mixing ratio (Briggs and Andrews 1980; de Pater and Gulkis 1988; Berge et al. 1988; Hofstader and

Muhleman 1989; Jaffe et al. 1984) is caused by a combination of dynamics and chemistry (i.e., polar downdrafts of NH_3-depleted gas and equatorial upwellings of NH_3-richer gas). Gulkis and de Pater (1984) had previously noted that the observed temporal (see, e.g., Gulkis et al. 1983; Klein and Turegano 1978) and latitudinal variations in the NH_3 mixing ratio might be related to each other. Also, Carlson et al. (1987*a*) and Hofstadfer and Muhleman (1989) proposed a similar model to account for the observed temporal and spatial variability in ammonia.

Thus a consensus appears to be emerging that both an enhancement of the Uranian H_2S/NH_3 ratio and a chemical mechanism for NH_3 loss are responsible for the inferred NH_3 depletion in the 150 to 200 K region of the atmosphere of Uranus. However, despite this consensus, several important problems remain unresolved. One significant problem is the different (and incorrect) thermodynamic data used to model NH_3 solubility in the aqueous solution clouds. As Table VI illustrates, this problem is especially acute at the high enrichment factors (thus leading to water cloud condensation at the critical point) favored by de Pater et al. (1989). At this temperature (647 K), the thermodynamic data used by de Pater et al. (1989), which are the same as those used by Romani (1986), underestimate NH_3 solubility by almost a factor of 3. (A similar problem is shared by Romani et al. [1989] who consider NH_3 depletion on Neptune.)

A second problem concerns the thermodynamic data used to calculate NH_4SH condensation via the reaction

$$NH_3(g) + H_2S(g) = NH_4SH(s) \tag{45}$$

which has been studied by Isambert (1881,1882), Magnusson (1907), and Walker and Lumsden (1897). Both Carlson et al. (1987*a*) and de Pater et al. (1989) have expressed concern about the accuracy of the available thermodynamic data and have noted that different compilations give different values for the enthalpy (ΔH) and entropy (ΔS) changes of Reaction (45). These different values lead to significant differences in the predicted NH_4SH cloud base temperatures. Thus, Fegley (1990*e*), who used Kelley's (1937) evaluation of the NH_4SH vapor pressure data of Isambert (1881,1882) and Walker and Lumsden (1897), calculated a cloud base temperature of 236 K for a solar composition model, while Romani (1986), who used the data tabulated by Wagman et al. (1965), calculated $T = 210$ K. Carlson et al. (1987*a*) calculated $T = 232$ K, in good agreement with Fegley (1990*e*). For reference, Table VII reproduces the results of Fegley (1990*e*) for NH_4SH condensation at various NH_3 and H_2S enrichments over solar composition.

Finally, a third problem with the "consensus model" for NH_3 depletion on Uranus involves the mechanism for enhancing the H_2S/NH_3 ratio. This mechanism is presumably related to the fact that sulfur is found as sulfide minerals (e.g., troilite FeS) in chondritic meteorites, while nitrogen is not

TABLE VII
NH_4SH Cloud Condensation on Uranus[a]

Enrichment Factor[b]	Cloud Base Temperature (K)
1.0	236
10	266
20	277
30	284
50	293
65	297

[a]Results from Fegley (1990*e*) who used Kelley's (1937) evaluation of the available vapor pressure data.
[b]Equal enrichments assumed for NH_3 and H_2S.

significantly incorporated into solid grains until much more volatile compounds and ices exemplified by NH_4HCO_3, $NH_3 \cdot H_2O$, $N_2 \cdot 6H_2O$, or $N_2(s)$ form (e.g., see Lewis and Prinn 1980). As a result the S/N atomic ratio in chondritic meteorites (S/N $\sim$ 10 in Type 1 carbonaceous chondrites) is significantly larger than the solar S/N ratio of $\sim$ 0.2. Thus, in principle, accretion of CI-chondrite-like material can provide the enhanced S/N ratios required by the "consensus model." However, the details of this scenario have not yet been worked out.

G. Gas Solubilities in Aqueous Clouds

Ammonia is not the only gas which can dissolve in the predicted aqueous solution clouds. As Table VIII indicates, nonpolar species such as H_2, CH_4 and He may also possess significant solubilities if water-cloud formation occurs near the critical point of 647 K. In fact, under these conditions, H_2 is predicted to be as soluble as NH_3 while CH_4 is even slightly more soluble. As Fegley and Prinn (1986) emphasized, the solubility of CH_4 provides a mechanism for depleting this gas above the water clouds. Furthermore, as noted by Stevenson (1984*b*) and by Fegley and Prinn (1986), the greater solubility of H_2 compared to that of He (approximately a factor of 20 at 647 K) provides a mechanism for enhancing the He/H_2 ratio above the water clouds. The predicted enhancement, which is on the order of a few percent, is potentially detectable by an entry probe. This mechanism may at least partially account for the (apparently) enhanced He/H_2 ratio on Neptune.

In addition to altering gaseous abundances above the water clouds, the dissolution of gases in the aqueous solution clouds also has important implications for phase equilibria (i.e., shifts in the critical point for the solution clouds) and thus for the cloud base condensation temperature. Experimental measurements (e.g., see Franck 1987; De Loos et al. 1980; Larsen and Prausnitz 1984; Seward and Franck 1981; Tsiklis et al. 1965) have determined the critical lines and show that the major gaseous solutes (H_2, He, CH_4 and NH_3)

TABLE VIII
Gas Solubilities in Water Clouds at 647 K[a]

Gas	Liquid-Phase Mole Fraction[b]
CH_4	0.10
H_2	0.09
NH_3	0.09
He	0.006
H_2S	0.006

[a]Table after Fegley and Prinn (1986).
[b]The liquid water mole fraction is 0.72. All other gases have mole fractions < 0.001.

present on Uranus all have an effect on the critical point of aqueous solution. This is schematically illustrated in Fig. 21 where it is seen that CH_4 and NH_3 decrease the critical point below the value for pure water, while H_2 only slightly increases it and He dramatically increases the critical point. At present, the exact phase equilibria in the $H_2O - H_2 - He - CH_4 - NH_3$ system are difficult to predict because of the lack of all relevant experimental data.

V. CONCLUSIONS

Recent Earth-based, Earth-orbital, and Voyager 2 observations have greatly increased our knowledge of the chemistry and spectroscopy of the atmosphere of Uranus over what was known two decades ago, prior to the modern era of spacecraft exploration of the solar system. During the coming

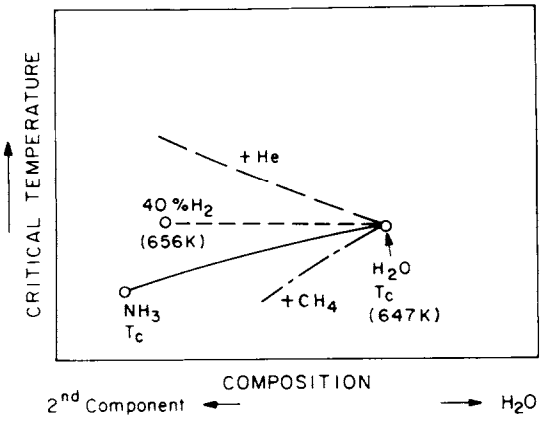

Fig. 21. A schematic diagram showing the effect of several possible dissolved gases on the critical temperature of water. Some solutes (CH_4, NH_3) decrease the critical temperature, while other solutes (H_2, He) increase the critical temperature. See the text for a full discussion (figure after Fegley 1990*d*).

years we can also look forward to continuing advances in our knowledge from the future use of the Hubble Space Telescope, continued improvements in Earth-based spectroscopic observations, new laboratory measurements of relevant kinetic, spectroscopic and thermodynamic data useful in interpreting spectroscopic observations, and the continued development of atmospheric models for the interpretation of spectroscopic data.

What are particularly interesting problems which advances in all of these areas may help to solve? One unresolved problem is the abundances of important condensible species such as H_2O, NH_3, and H_2S in the lower troposphere of Uranus. Although the Voyager 2 encounter was successful in determining the H_2, He, and CH_4 abundances in the upper troposphere of Uranus, we still have no direct observations of H_2O, NH_3 and H_2S. (Indeed, at this time water vapor has only been observed on Jupiter; NH_3 has only been observed on Jupiter and Saturn; and H_2S has not yet been observed on any of the giant planets.)

The Ne/H_2 mixing ratio is also of interest because Ne is not trapped in ices or clathrates and should not be enriched (relative to H_2) the way carbon is (Gautier and Owen 1989). This hypothesis needs to be verified, however, as it is linked to models for formation of the planet. Like the N_2 abundance determination discussed earlier, a neon abundance determination will require the use of a mass spectrometer on an atmospheric entry probe. In this case, the $^{20}Ne/^{22}Ne$ ratio could also be determined and compared to the value that Galileo is expected to determine for Jupiter and to the plethora of meteoritic determinations.

Further progress is also needed to measure the isotopic ratios of other major elements. Most important is an unambiguous determination of the D/H ratio in H_2 gas. The deuterium enrichment that has been detected in CH_4 should be expressed in H_2 as well. As mentioned earlier, a D/H measurement in both H_2 and CH_4 would also allow an empirical determination of the methane fractionation factor. Since HD observations in the visible and near-infrared regions are not feasible (see Sec.III.B.5) it appears that an HD abundance determination will have to be made using the rotational spectrum in the microwave (extremely difficult owing to the lower thermal luminosity of Uranus) or again with an entry probe. The $^{12}C/^{13}C$ ratio also needs to be evaluated and some progress may be expected from Earth-based observations before an *in situ* measurement is made from a probe. If either N_2 or NH_3 is present in sufficient abundance, the mass spectrometer on an entry probe will also be able to measure $^{14}N/^{15}N$.

In the stratosphere, we confront a separate set of problems. Voyager 2 demonstrated that chemical reactions are taking place, producing substances that absorb light in the ultraviolet (Smith et al. 1986; Pollack et al. 1987). Given our experience at Titan (see, e.g., Strobel 1982), it seems virtually certain that intermediate products along the chain of reactions that leads from CH_4 (and possibly N_2) to the ultraviolet absorbing aerosols should be detect-

able. Indeed, as discussed in the chapter by Atreya et al., C_2H_2 has been found with a mixing ratio of 10^{-8} (Caldwell et al. 1981; Broadfoot et al. 1986; Orton et al. 1987; Caldwell et al. 1988). As Earth-based systems improve over the next few years, one may expect additional molecules to be discovered. The detection of nitriles would be especially interesting, in that it would signal the presence of N_2 in the stratosphere.

Given the remarkable orientation of the planet's rotational axis and the lack of a strong internal heat source, one might well expect seasonal variations in the visible region of the atmosphere. Lockwood et al. (1983) have already detected such changes in the albedo. Thus it would be particularly fruitful to repeat the suite of groundbased observations that led to the present model during the epoch around 2006 when the equator of Uranus is facing the Sun.

Finally, the launch of the Hubble Space Telescope (HST) offers the possibility of investigating the near ultraviolet spectrum of Uranus with unprecedented resolution and signal-to-noise. These observations will allow much improved searches for simple polyacetylenes, CO, N_2H_4 and other trace gases in the ultraviolet. When SIRTF, SOFIA, and infrared instrumentation on HST become available, one can anticipate similar leaps forward in the infrared.

Acknowledgments. B. Fegley thanks the NASA Planetary Atmospheres Program for supporting his research on the chemistry of the outer planets from Nov.1986 to Nov.1989. His research on outer planet chemistry during Nov.1989 to Dec.1990 has been supported by the Max-Planck-Institute für Chemie. T. Owen thanks the NASA Planetary Atmospheres Program and the Voyager Project for their support. He also wishes to thank W. Hubbard for helpful discussions. B. Fegley gratefully acknowledges assistance from M. Ashton, H. Hansen, C. Sobon, and of G. Feyerherd and J. Bambach as well as the staff and students of the Max-Planck-Institut.